# CARRIER PROPAGATION ON THE SHIRORO COMPLEX 132kV TRANSMISSION LINES

**BY**

**ADEGBOYE BABATUNDE ARAOYE**

A Thesis Presented to the Department of Electrical Engineering, Ahmadu Bello University, Zaria in Partial Fulfillment of the Requirements for the Award of the Master of Science (M.Sc .) Degree in Electrical Engineering with Specialization in Electronics and Telecommunications.

**OCTOBER, 1996.**

# DECLARATION

I hereby declare that this thesis has been executed by me and that it is a record of my research work. It has not been submitted or accepted in any previous publications for a higher degree. All sources of information have been specifically acknowledged by means of references.

ADEGBOYE, Babatunde Araoye

Date: 19/11/96

# CERTIFICATION

This Thesis entitled "CARRIER PROPAGATION ON THE SHIRORO COMPLEX 132kV TRANSMISSION LINES" by ADEGBOYE, Babatunde Araoye, meets the Regulations governing the Award of the Degree of Master of Science (M.Sc.) of Ahmadu Bello University, Zaria, and is approved for its contribution to knowledge and literary presentation.

Dr. B.G. Ishaku
Chairman,
Supervisory Committee

Date: 23-1-97

Dr. M.A. Gulma
Head, Electrical Engineering
Department

Date: 23-1-97

Dean of Postgraduate School

Date: 15/12/97

# DEDICATION

To the Entire Family of Deacon J.K. Adegboye

*May His Blessings be Upon This*
*Family in Jesus Name*
*And To Him Be All*
*Glory Forever.*
Amen.

# ACKNOWLEDGMENTS

The Lord is my strength and my shield; in Him my heart trusts (Ps. 28:7)..... In all your ways, acknowledge Him and He shall make your path straight (Prov. 3:5-6).... For nothing is impossible before God (Mark 10:27). I sincerely acknowledge God for making everything possible.

I am greatly indebted to my supervisor, Dr. B.G. Ishaku, who, despite his numerous commitments, gave me the opportunity of working under him and for his valuable advice, constructive criticisms and fatherly role throughout the programme.

I wish to express my gratitude to Dr. Z.O. Oyedokun, the former Head of Department throughout the period this manuscript was written. I thank the present Head of Department, Dr. M.A. Gulma along with his staff in the academic, technical as well as the administrative side, for their support and cooperation during the course of this project. I fervently pray that God will reward each and everyone of them accordingly.

My sincere appreciation goes to the entire management of the 330/132/33kV substation of NEPA, Mando, Kaduna, especially Engr. Joe Ndiagwalukwe (Senior Manager, PC&M), Mr. John Obajulu (Manager, PC&M), Mr. Durotola of the 132kV transmission station, Abuja, Alh. Isa Ajia (Manager, S/O), Mr. S. Mustapha (Asst. Manager, Communications) and others that have contributed in one way or the other.

My thanks also go to Dr. J. O. Afolayan of Civil Engineering Department, Tunmise Opatola and David Barau, both of Electrical Engineering Department, Ahmadu Bello University, Zaria. I wish to thank my best friend and colleague, S. G. Abdullahi, for the wonderful role he played in the course of this project; .....the reward of humility and fear of the Lord is riches and honour in life (Prov. 22:4).

Worth mentioning also is Mr. Abdul B. Kareem, who has always been standing by me in my work and in all the phases of the programme. May God in His Infinite Mercy reward you and your family accordingly.

I sincerely acknowledge my aunt, Mrs. D. A. Ojumoola and her family for their moral and spiritual supports and finally, my fervent regards go to Mr M. F. Forsyth, the head of the Computer Studies Department, Kaduna State Polytechnic, Zaria for making his machine available for use and also for transforming this manuscript to a beautiful thesis.

Adegboye, B. A.
Assistant Lecturer,
October, 1996

# ABSTRACT

This project aims at assessing the carrier propagation on a specified section of NEPA overhead powerlines, namely, the Shiroro Complex 132kV lines.

Following an overview discussion of powerline carrier communication systems, consideration was given to the type of parameters required for assessing the communication system on the Shiroro Complex.

Line parameters obtained from the Kaduna 330/132/33kV transmission station were used to determine the basic series impedance and shunt admittance matrices of the network. The parameters for electrically short lines at power frequency and those for the electrically long lines at higher frequencies were then derived from the matrices.

The results were analysed and conclusions drawn from the analysis. Finally, some recommendations were presented for possible use by the management of NEPA and also for further work.

# TABLE OF CONTENTS


Title ..... i
Declaration ..... ii
Certification ..... iii
Dedication ..... iv
Acknowledgements ..... v
Abstract ..... vi
Table of Contents ..... vii
List of Tables ..... ix
List of Figures ..... x
Symbols and Abbreviations ..... xi

**CHAPTER ONE - INTRODUCTION**

1-1 Thesis Motivation ..... 1
1-2 Literature Review ..... 1
1-3 Problem Formulation and Methodology ..... 3
1-4 Thesis Outline ..... 3

**CHAPTER TWO - POWERLINE COMMUNICATIONS SYSTEM COMPONENTS AND ANALYSIS**

2-1 Introduction ..... 5
2-2 Powerline Carrier Equipment ..... 6
2-2-1 Coupling Capacitor ..... 6
2-2-2 Line Trap Unit ..... 7
2-2-3 Tuning Devices ..... 8
2-2-4 Method of Coupling ..... 8
2-3 Carrier Communications ..... 8
2-3-1 Single-Frequency Manual - Simplex System ..... 10
2-3-2 Two-Frequency Duplex System ..... 10
2-3-3 Modulation Systems ..... 10
2-3-4 Amplitude Modulation ..... 10
2-3-5 Frequency Modulation ..... 11
2-3-6 Single Sideband ..... 11
2-3-7 Calling Systems ..... 12
2-4 Calculation of the Basic Matrices ..... 12
2-4-1 Calculation of the Admittance Matrix ..... 12
2-4-2 Calculation of the Impedance Matrix ..... 14
2-4-3 Reactance due to Physical Geometry ..... 15
2-4-4 Effect of Earth-Return Path ..... 15
2-4-5 Components due to Conductors ..... 16
2-4-6 Effect of Earth Wires in Impedance Matrix ..... 17
2-5 Calculation of Derived Parameters ..... 17
2-5-1 Parameters for Electrically Short Lines ..... 17

2·5·2 Parameters for Electrically Long Lines ..... 19

## CHAPTER THREE - COMPUTER-AIDED DATA ANALYSIS

3·1 Introduction ..... 22
3·2 Data ..... 25
3·2·1 Determination of Input Data for High Frequency Calculations (HFC) ..... 26
3·2·2 Determination of Conductor Input Parameter for HFC ..... 26
3·2·3 Determination of Earth Wire Input Parameters for HFC ..... 27
3·2·4 Determination of Input Data for Power Frequency Calculations (PFC) ..... 27
3·2·5 Determination of Conductor Input Parameters for PFC ..... 27
3·2·6 Determination of Earth Wire Input Parameters for PFC ..... 28
3·3 Input Data for HFC ..... 28
3·3·1 Conductor Input Data for HFC ..... 28
3·3·2 Earth Wire Input for HFC ..... 29
3·4 Input Data for PFC ..... 29
3·5 Program and Results ..... 29
3·5·1 The program ..... 29
3·5·2 Analysis of Results ..... 40

## CHAPTER FOUR - CONCLUSIONS AND RECOMMENDATIONS

4·1 Conclusions ..... 50
4·2 Recommendations ..... 51
References ..... 53

## APPENDICES

A Line impedances for Kaduna Region 132 kV circuits ..... 56
B Line parameters for Shiroro Complex 132 kV lines ..... 57
C Configuration of Shiroro Complex 132 kV line ..... 58
D Program PLC_SHIR ..... 59
E Map of Nigeria showing the NEPA grid system (Shiroro Complex highlighted) ..... 71
F System flow sheet for Kaduna region ..... 72

# LIST OF TABLES


3·1 Line Impedances for Kaduna Region 132kV Circuits ..... 23
3·2 Line Parameters for Shiroro Complex 132kV Line ..... 24
3·3 Derived Parameters for Electrically Long Lines at 1kHz Frequency ..... 42
3·4 Derived Parameters for Electrically Long Lines at 10kHz Frequency ..... 43
3·5 Derived Parameters for Electrically Long Lines at 100kHz Frequency ..... 44
3·6 Derived Parameters for Electrically Long Lines at 1MHz Frequency ..... 45
3·7 Derived Parameters for Electrically Short Lines at Power Frequency ..... 46

# LIST OF FIGURES


| | | |
|---|---|---|
| 2·1 | Schematic Diagram of a Power-Line Carrier Equipment | 5 |
| 2·2 | Schematic Diagram of the Coupling Capacitor | 7 |
| 2·3 | Schematic Diagram of a Single-Frequency Line Trap | 7 |
| 2·4 | Line-to-Ground Method of Coupling | 9 |
| 2·5 | Line-to-Line Method of Coupling | 9 |
| 2·6 | Single-Frequency Manual - Simplex System | 10 |
| 2·7 | Two-Frequency Duplex System | 11 |
| 2·8 | Schematic of Conductors | 13 |
| 2·9 | Series Symmetrical - Component Equivalent Circuit for Electrically Short Lines | 20 |
| 2·10 | Shunt Symmetrical - Component Equivalent Circuit for Electrically Long Lines | 20 |
| 3·1 | Configuration of the Shiroro Complex 132kV Lines | 25 |
| 3·2 | Flow Chart for the Block Program | 30 |
| 3·3 | Structure Chart for the Structured Program | 38 |
| 3·4 | Variation of Attenuation with Frequency | 47 |
| 3·5 | Variation of Velocity Difference with Frequency | 48 |
| 3·6 | Variation of Attenuation with Velocity Difference | 49 |

# SYMBOLS AND ABBREVIATIONS

| | | |
|---|---|---|
| **B** | - | charge coefficient matrix |
| **C** | - | sequence capacitance |
| CSA | - | cross sectional area |
| $d_{ij}$ | - | distance between conductor i and conductor j |
| $D_{ij}$ | - | distance between conductor i and image of conductor j |
| HFC | - | high frequency calculations |
| **i** | - | identity matrix |
| **I** | - | conductor current matrix |
| NEPA | - | National Electric Power Authority |
| p | - | number of circuits |
| PFC | - | power frequency calculations |
| q | - | number of earth wires |
| **Ψ** | - | conductor charge matrix |
| **R** | - | series resistance matrix per unit length |
| **X** | - | series reactance matrix per unit length |
| **Y** | - | shunt admittance matrix per unit length |
| **Z** | - | series impedance matrix per unit length |
| **P** | - | matrix obtained by multiplying **Z** and **Y** |
| $\mathbf{P}_e$ | - | real correction component matrix |
| $\mathbf{Q}_e$ | - | immaginary correction component matrix |
| **S** | - | eigenvector matrix of **P** |
| **V** | - | conductor voltage matrix |
| $\mathbf{Y}_0$ | - | characteristic impedance matrix |
| Z | - | sequence impedance |
| $\mathbf{Z}_0$ | - | characteristic impedance matrix |
| λ | - | eigenvalue matrix of **P** |
| γ | - | diagonal propagation matrix |
| $\theta_{ij}$ | - | angle subtended at conductor i by image of conductor i and image of conductor j |
| ε | - | permittivity |
| μ | - | permeability |
| ρ | - | resistivity |
| ω | - | angular frequency |

# CHAPTER ONE

# INTRODUCTION

## 1.1 THESIS MOTIVATION

With the ever increasing interconnections and complexity of a power system network and the need for transferring large amounts of power at extra high voltages, it has become necessary to monitor and control the various states of a power system at various important locations for the load despatch centre. One of the means of achieving this is by employing the powerline carrier channel. The powerline carrier is a term used to describe the significant use of carrier current communications when utilising the high voltage transmission line as the medium of propagation. Carrier current is a means of communication where the transmitted information is chanelled through a transmission medium which may also be in the form of an ordinary cable or coaxial cable.

Powerline carrier facilities are used primarily to provide company-owned communication services for power system operation. On large power systems, it is not possible to provide all the communication needs of the company by means of a powerline carrier because of the limited frequency spectrum available. Nevertheless, high-voltage transmission lines do provide a very reliable medium for communication for essential services in large power systems as well as for all the needs of smaller power systems.

The use of the powerline carrier is also justified because of the economy involved when communication is required between adjacent substations for voice communication, telemetering, protective relaying and so on.

## 1.2 LITERATURE REVIEW

The determination of powerline carrier attenuation by calculation can best be regarded as an estimate because of the individual peculiarities which exist on any line due to many factors for which consistent predicting methods are yet to be formulated. In order to be sure of proper powerline operation, measurements of carrier frequency response, that is, attenuation versus frequency, should be made on all newly installed carrier channels. Examples of poor frequency response include very narrow bandwidth for required carrier service and periodic or erratic variations of attenuation versus frequency. Some problems that could adversely affect the powerline operation include bad weather, reflections, line configuration, tap lines and multiple path transmission.

Bad weather increases attenuation on transmission lines, so also do environmental contaminants. Other problems that could hinder proper operation of powerline carrier include reflections, due to nonuniformity of line characteristics at towers and variable conductor heights above uneven terrain. Line configuration changes also do cause severe reflections.

Tap lines and multiple path transmission also present real problems. It should be noted that small differences in velocity between modes of similar attenuation may result in abnormally high attenuation for certain conditions of energization of carrier coupling. This is due to the fact that the method of energization is directly related to the frequency and line length. Also, attenuation increases more steeply at higher frequencies in multiconductor powerlines with much wider proportionate spacing, so that it is more nearly a linear function of frequency than parabolic.

Studies to determine the effects of ice on loss characteristics of intrabundle and conventional powerline carrier channels were carried out by Wasley [1]. The effects of tap lines without carrier traps on the carrier attenuation was lucidly discussed by Belous et al [2]. These two authors as well as Senn and Morf [3] have considered the effect of transposition on carrier attenuation. The effect of sag and insulation capacitance and resistance have been taken into account by Perelmen [4] and Zakar-Itkin [5]. Although Zakar-Itkin considered the effect of sag on carrier attenuation based on a continuous variation of the line parameters, the results were not compared to those in which the effect of sag was ignored. Therefore, Zakar-Itkin's study does not provide the means of estimating how far the sag influences the carrier attenuation.

Effects of earth resistivity on the modal parameters of an extra high voltage horizontal line at powerline carrier frequencies was studied by Perz et al [6] and has been extended to a twin-bundle conductor line by Indulkar et al [11]. Christina et al [7] developed a sensitivity model to compute the partial derivatives of the carrier channel attenuation coefficient with regard to numerous line and earth parameters. In [8], a mathematical model to evaluate the carrier channel performances on lossy nonuniform, multiconductor transmission lines was presented by Christina and D'Amore. Wedepohl [9] developed matrix methods for solving travelling-wave phenomena in a polyphase system. These methods were used for the calculation of electrical parameters for short and long polyphase transmission lines [10]. Indulkar et al [11] also studied the effectiveness of a carrier channel on a powerline under various power frequency load conditions.

## 1·3 PROBLEM FORMULATION AND METHODOLOGY

A knowledge of multiconductor transmission line parameters is necessary in analysing a number of power transmission problems. These parameters may be divided into two groups, namely, those at power frequency, which are required in order to study load flow, system stability and fault levels, and those at higher frequencies, which are needed for studying the effects of restriking voltages, switching overvoltages, radio interference and the propagation characteristics of powerline carrier signals.

In this thesis, however, the study of the propagation characteristics would be of interest. The objective is to study among others, the signals attenuation on the lines at high frequencies as well as the velocities at which such signals are propagated. The frequencies would be between the range of kilohertz (kHz) and megahertz (MHz). From a careful assessment, one would be able to observe the frequencies at which significant power would be obtained at the receiving end of the lines. The thesis would also present the power frequency parameters.

Present transmission lines are electrically short at power frequency. Consequently, it is usually permissible to calculate series and shunt parameters separately. This separation is not possible at higher frequencies. Hence, the problem must be solved in terms of wave propagation parameters [9]. A digital computer program would, however, be used to trim down the complexity of the mathematical expressions involved in multiconductor line problems. The basic series impedance, Z and shunt admittance, Y matrices will be developed and manipulated practically. These matrices which define the parameters of electrically short lines may be expressed in terms of symmetrical components when asymmetry of the line can be neglected.

For electrically long lines, a method of calculating the modal parameters of the lines which is based on a solution to the wave equation [9] will be adopted. This method in turn, is based on the evaluation of the eigenvalues and eigenvectors of a complex matrix derivable from the basic system matrices.

## 1·4 THESIS OUTLINE

The thesis is divided into five chapters. Chapter One gives a general introduction of the project work. The second chapter presents the essential parts and components of the powerline carrier communications system. The chapter also presents the modulation systems employed by the powerline

carrier and discusses the analytical approaches to carrier propagation on overhead power lines.

Chapter Three presents the data obtained from NEPA, the data computed for analysis as well as the computer-aided analysis of the data. The chapter also analysed the results obtained.

Finally, Chapter Four gives the conclusions drawn from the results obtained and presents some recommendations which may be found useful by the management of NEPA, as well as for further work.

# CHAPTER TWO

## POWERLINE COMMUNICATIONS SYSTEM COMPONENTS AND ANALYSIS

### 2·1 INTRODUCTION

Electrical Power Transmission Lines are used extensively for communication purposes. In such systems, transmission of intelligence takes place simultaneously with the transmission of electrical energy and without mutual interference.

The Powerline carrier consists of a band of frequencies between 30 and 500 kilohertz, which is transmitted over a powerline. The carrier frequency band is divided into suitable channels, for use for

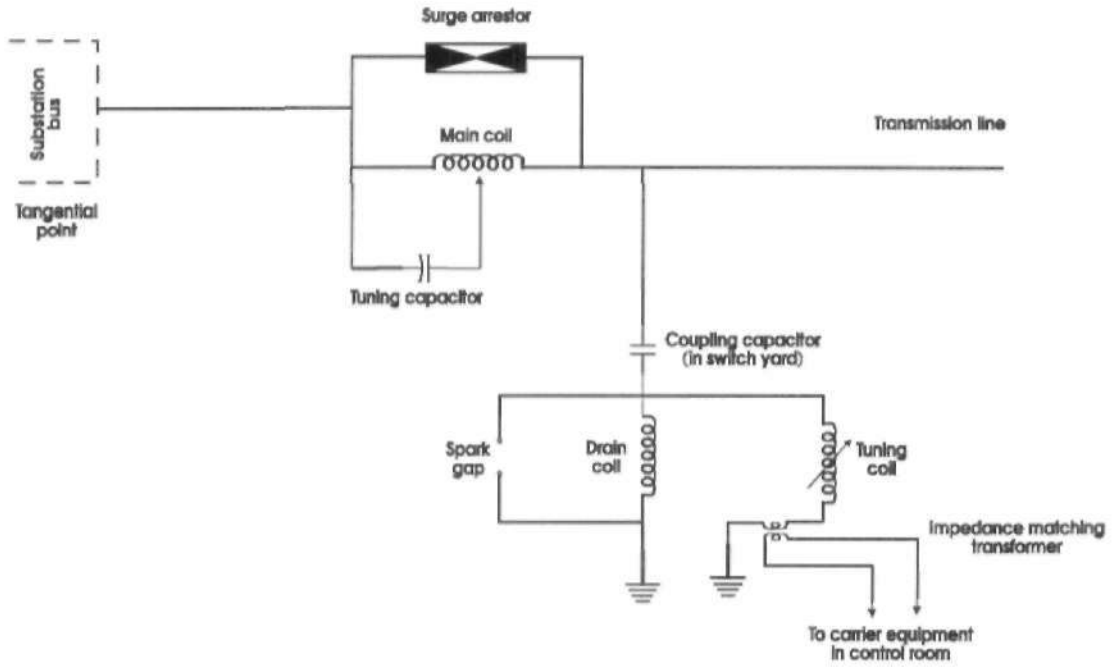



*Fig 2·1: Schematic diagram of a powerline carrier equipment*

voice communication, protective relaying, telemetering, load control and supervisory control. The high frequency signals are transmitted through the powerlines and the carrier current equipment comprises coupling capacitors, line traps, tuning devices, and so on. Fig. 2·1 shows a schematic diagram of a typical powerline carrier equipment.

The multiconductor transmission-line theory is well developed and, is applicable to both power and communication lines. Attenuation is a measure of the energy lost when intelligence is transferred from the transmitting terminal to the receiving terminal. This loss is dependent on the line configura-

tion, frequency, conductor size, presence and type of earth wires, transposition, earth resistivity and the weather condition.

The attenuation of a carrier channel over a power transmission line can be determined by using the series-impedance and shunt-admittance matrices per unit length of the line. These matrices give the electrostatic and electromagnetic performance of the line and therefore depend on the physical and electrical characteristics of the lines, their geometrical arrangement and height above the ground level.

The propagation characteristics of the transmission line can be predicted by a method known as the modal analysis. This method provides accurate prediction of the line attenuation provided that end effects and reflections are negligible. The modal analysis is analogous to the symmetrical components used to calculate the short circuit currents during fault conditions on the power transmission line. The only difference lies in the operator matrix. Modal analysis assumes the natural modes of propagation of voltage and current associated with the carrier signals transmitted on the lines. The modes are represented by a characteristic impedance, constant attenuation and the propagation velocity.

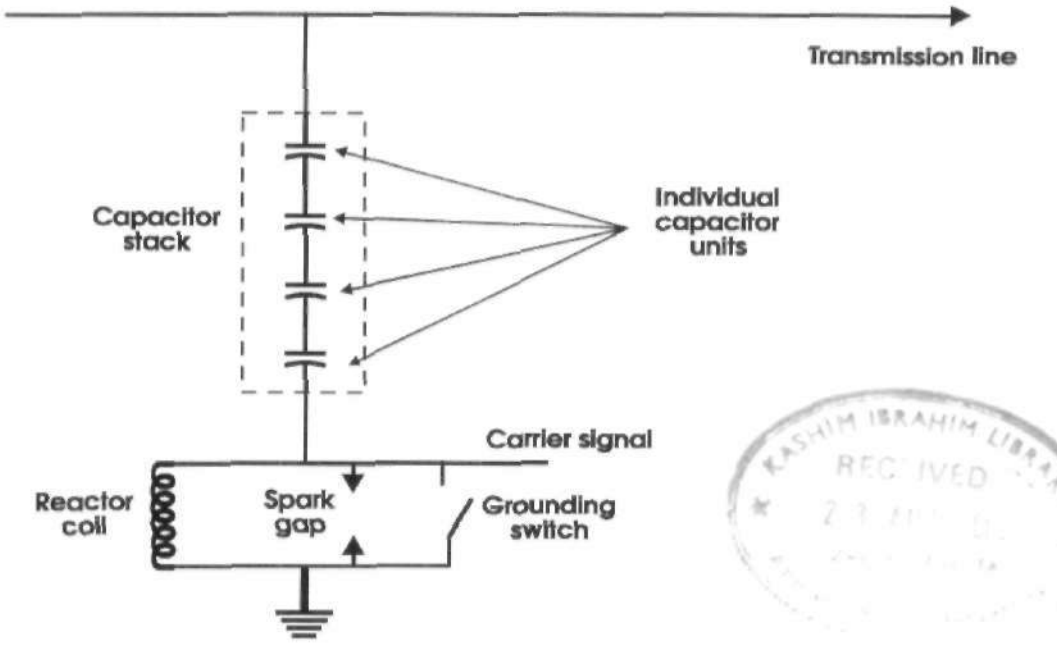
The accuracy of the results depends on how close the mathematical expressions for the basic series impedance and shunt admittance matrices are to reality. The formation of ideal impedance and admittance matrices of a real transmission line should consider the actual physical layout of the line only and not on any assumptions about the geometrical layout of the conductors, the electrical properties of the conductor materials or the earth resistivity.

The natural mode concept which is helpful in predicting the distribution of carrier-frequency current among the power conductors is also useful in explaining many apparently strange aspects of the carrier behaviour. A transmission line with n conductors has n natural modes which, when combined in appropriate proportions, can represent any current or voltage distribution among the n wires.

## 2.2 POWER LINE CARRIER EQUIPMENT

### 2.2.1 Coupling Capacitor

The Coupling Capacitor allows carrier frequency signals to enter the carrier equipment but opposes the 50Hz power frequency current from entering the carrier equipment which is connected to the transmission line. To further reduce the impedance, an inductor of low inductance is connected in




KASHIM IBRAHIM LIBRARY
RECEIVED

*Fig 2.2: Schematic diagram of the coupling capacitor*

series with the coupling capacitor to form a resonant circuit at carrier frequency. Fig. 2.2 shows a schematic diagram of a typical coupling capacitor.

### 2.2.2 Line Trap Unit

The line trap unit is a parallel tuned circuit comprising an inductor, L and a capacitor, C and is inserted between the busbar and the connection of the coupling capacitor to the line. Line traps have

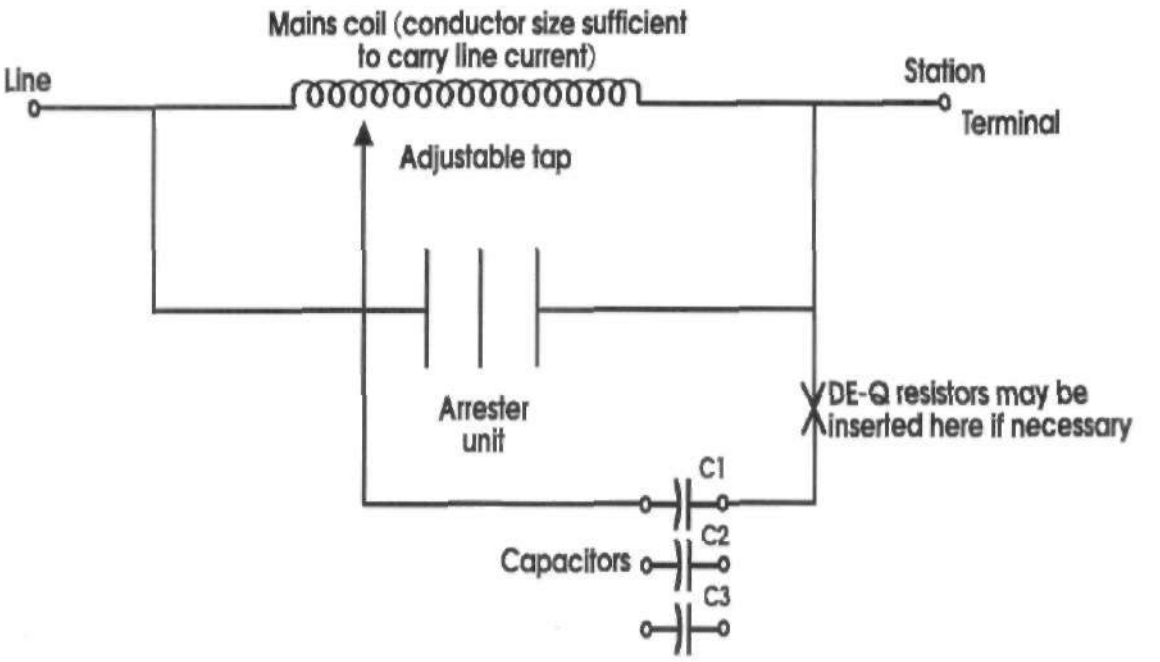



*Fig 2.3: Schematic diagram of a single frequency line trap*

negligible impedance at power frequency and therefore do not affect normal power current. They provide a means of confining the major portion of the carrier energy to its intended path and of isolating sources of high attenuation from the carrier circuit. Fig. 2.3 shows a schematic diagram of a typical single-frequency line trap. The function of the DE-Q resistor is to reduce the peak impedance of the line trap thereby reducing distortion on wideband channels such as FM telephone carriers.

### 2.2.3 Tuning Devices

At carrier frequencies, the load resistance presented by powerlines ranges from 400 to 900 ohms. The reactance of coupling capacitors, effectively in series with this load, are appreciable and must be compensated for if maximum coupling efficiency and a resistive load condition for the carrier transmitter are to be obtained. This compensation can be achieved by placing in series with the coupling capacitor, an inductor whose inductance can be varied so that its reactance cancels that of the coupling capacitor at the carrier frequency.

The main function of a line-tuning device therefore is to furnish an adjustable inductance to cancel out the coupling capacitor reactance at carrier frequency. There are three types of line-tuning devices, namely, the single-frequency, double frequency and the broadband.

### 2.2.4 Method of Coupling

The simplest and most popular way of utilizing one or more conductors of a three-phase power line is to use one conductor of the powerline as one leg of the carrier circuit with ground return as the other path. This system, referred to as *line-to-ground* coupling is shown in Fig. 2.4 and requires the least amount of coupling elements in the form of coupling capacitors, line traps and line tuners.

In cases where the ground characteristics are unfavourable or where the transmission line is quite long, less carrier signal attenuation and a better signal to noise ratio can be obtained by using *line-to-line* coupling as shown in Fig. 2.5. The line tuning unit used with the line-to-line method of coupling has two variable inductances, one being used for each of the coupling capacitors.

## 2.3 CARRIER COMMUNICATIONS

A powerline carrier communications system can be classified as simplex or duplex depending on its mode of operation. Only one carrier frequency is used in a simplex carrier unit, and only one terminal transmits at a time since the transmitter blocks the local receiver. A simplex system is,

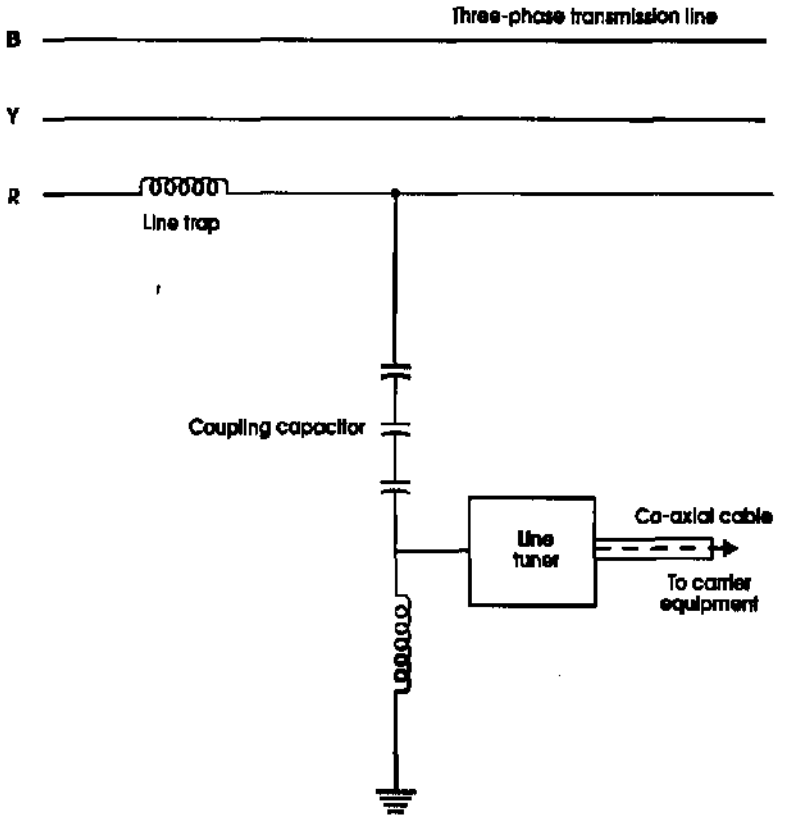



*Fig 2 4: Line-to-ground method of coupling*

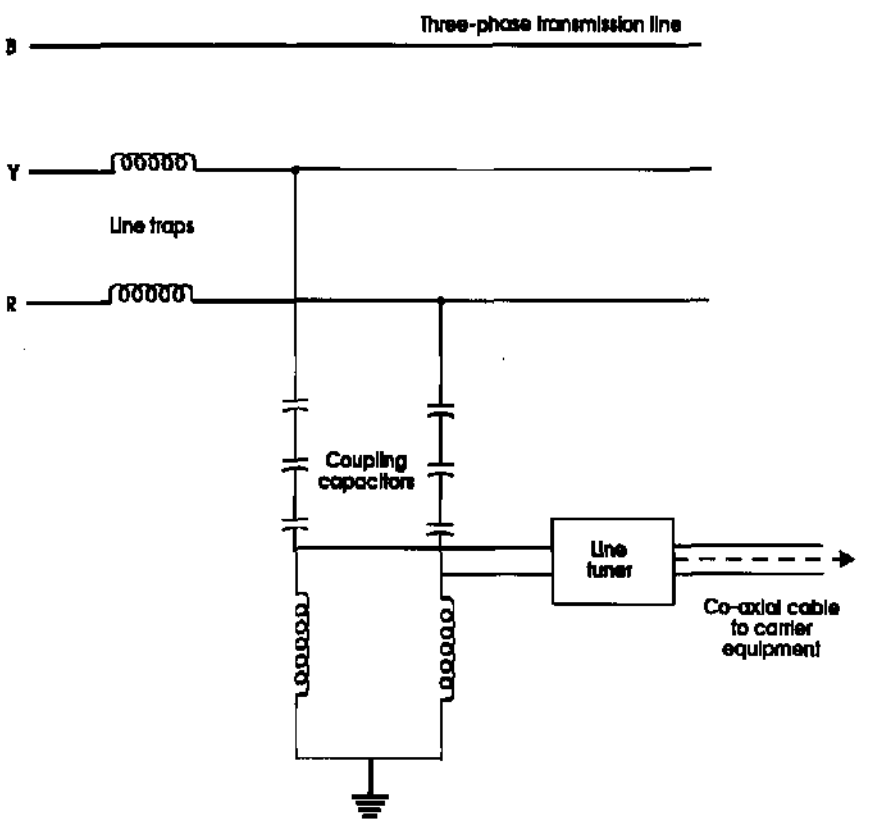



*Fig 2 5: Line-to-line method of coupling*

therefore, a *push-to-talk* system. In the duplex system, continuous transmission of a carrier from each terminal is made possible through the use of separate frequencies for the two directions.

### 2·3·1 Single-Frequency Manual-Simplex System

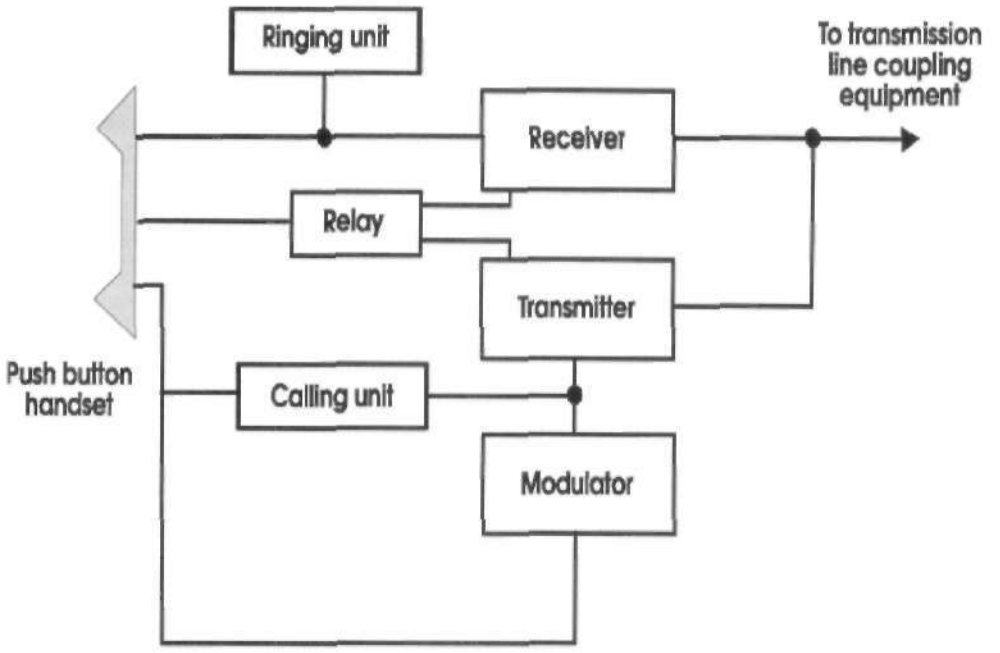



*Fig 2·6: Single-frequency manual simplex system*

This system is shown in Fig. 2·6 where *send-receive* switching operations are performed by the operator with a push button on the telephone handset.

### 2·3·2 Two-Frequency Duplex System

The basic units of this system are shown in Fig. 2·7. Besides the fact that the transmitter and receiver operate at different frequencies, the most important difference between this system and the simplex system is the addition of the *audio hybrid unit*, which makes it possible for the transmitter and receiver to operate continuously during conversation without switching operations.

### 2·3·3 Modulation Systems

The three modulation systems that are employed in powerline carrier communications applications are amplitude modulation, AM, frequency modulation, FM, and single sideband system, SSB.

### 2·3·4 Amplitude Modulation

The amplitude modulation used in powerline carriers is basically the same as that used in the standard broadcast band of commercial radio. It is the most vulnerable of all systems to atmospheric

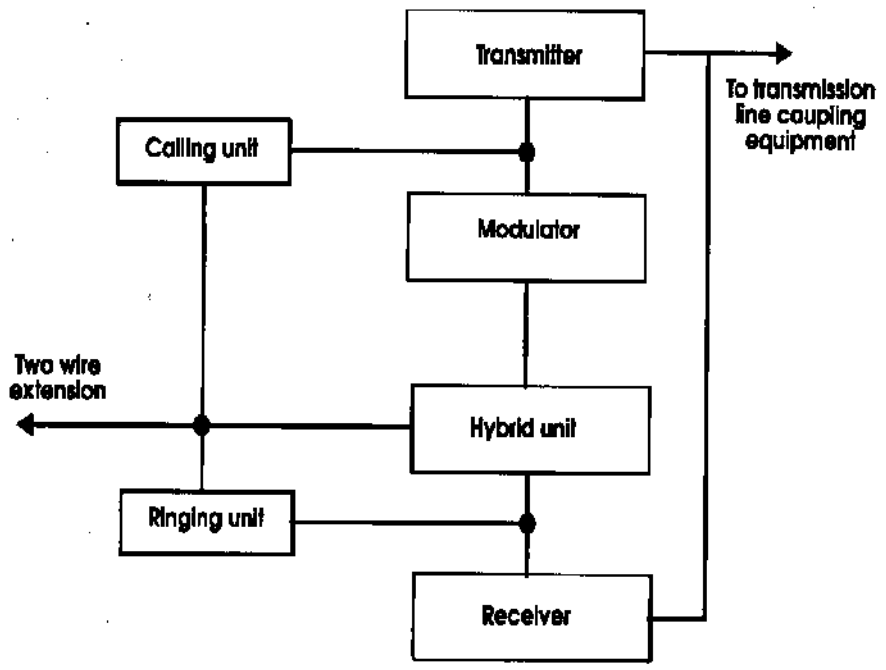



*Fig 2.7: Two-frequency duplex system*

and other line noises.

### 2.3.5 Frequency Modulation

The frequency modulation used in powerline carriers is of the narrowband type in order to conserve space in the frequency spectrum. Noise encountered on powerlines affects the amplitude of a received signal. Therefore, FM systems inherently offer an advantage over amplitude-modulated systems in that FM are more immune to noise.

### 2.3.6 Single Sideband

This is a form of amplitude modulation which requires only one-half the bandwidth of an AM or FM system transmitting the same audio-frequency range. The intelligence may represent the entire transmitter power output even though, the normally suppressed carrier is reinserted at a reduced level to be used for synchronizing or regulating purposes at the receiver, in some single sideband transmitters.

Since the single sideband receiver does not require the presence of a continuous carrier in the received signal, it can receive intelligible signals from more than one source simultaneously by reinserting one carrier to demodulate all signals. This principle is utilized in single sideband equipment to provide party-line operation of duplex equipment. A repeater is used at intermediate points which

transmits the same band of frequencies in each direction and likewise receives the same from each direction

### 2-3-7 Calling Systems

Different methods of establishing a call over a carrier channel exist. The simplest of these uses the presence of the carrier wave at the receiver to actuate a relay to ring a bell, light a lamp, and so on. This system is commonly used with the simplex communication circuits.

In the duplex system, transmitters are normally on and the carrier is present at all times. Calling on this system is accomplished by using *calling units* and *ringing units*.

The calling unit modulates the transmitter with a low frequency, usually 20Hz. At the receiving end, the carrier wave is demodulated and the 20Hz operates the ringing unit, actuating a relay to ring a bell or light a lamp as appropriate.

The calling system is compatible with a conventional private branch exchange (PBX) equipment and automatic dialing, selective code ringing, and so on, can be provided.

## 2-4 CALCULATION OF THE BASIC MATRICES

A multiconductor line is defined by its series-impedance matrix, **Z** per unit length and its shunt-admittance matrix, **Y** per unit length. These matrices are calculated from basic line data.

### 2-4-1 Calculation of the Admittance Matrix

The admittance matrix, **Y** is a function only of the physical geometry of the conductors relative to the earth plane, because the conductor and earth surfaces may each be regarded as equipotential surfaces. Since the conductance of the air path is negligible, **Y** has no real part. The physical location of the conductors is defined with respect to a coordinate system, with the earth plane as horizontal reference axis and the axis of symmetry of the tower as vertical reference.

From the coordinates of the conductors and conductor radii, elements of a matrix **B** are calculated with the i, j$^{th}$ element defined as [9]:

$$\mathbf{B} = \left[B_{ij}\right] = \log_e\left(\frac{D_{ij}}{d_{ij}}\right) \qquad (2\text{-}1)$$

where, $d_{ij}$ is the distance between the i$^{th}$ conductor and the j$^{th}$ conductor for $i \neq j$ and is the radius of

the $i^{th}$ conductor for i = j, and $D_{ij}$ is the distance between the $j^{th}$ conductor and the image of the $i^{th}$ conductor.

This is shown schematically in Fig. 2·8. The values of $d_{ij}$ and $D_{ij}$ can be found by applying trigonometrical equations as follows:

$$d_{ij} = \sqrt{\left(x_i - x_j\right)^2 + \left(y_i - y_j\right)^2} \qquad (2 \cdot 2)$$

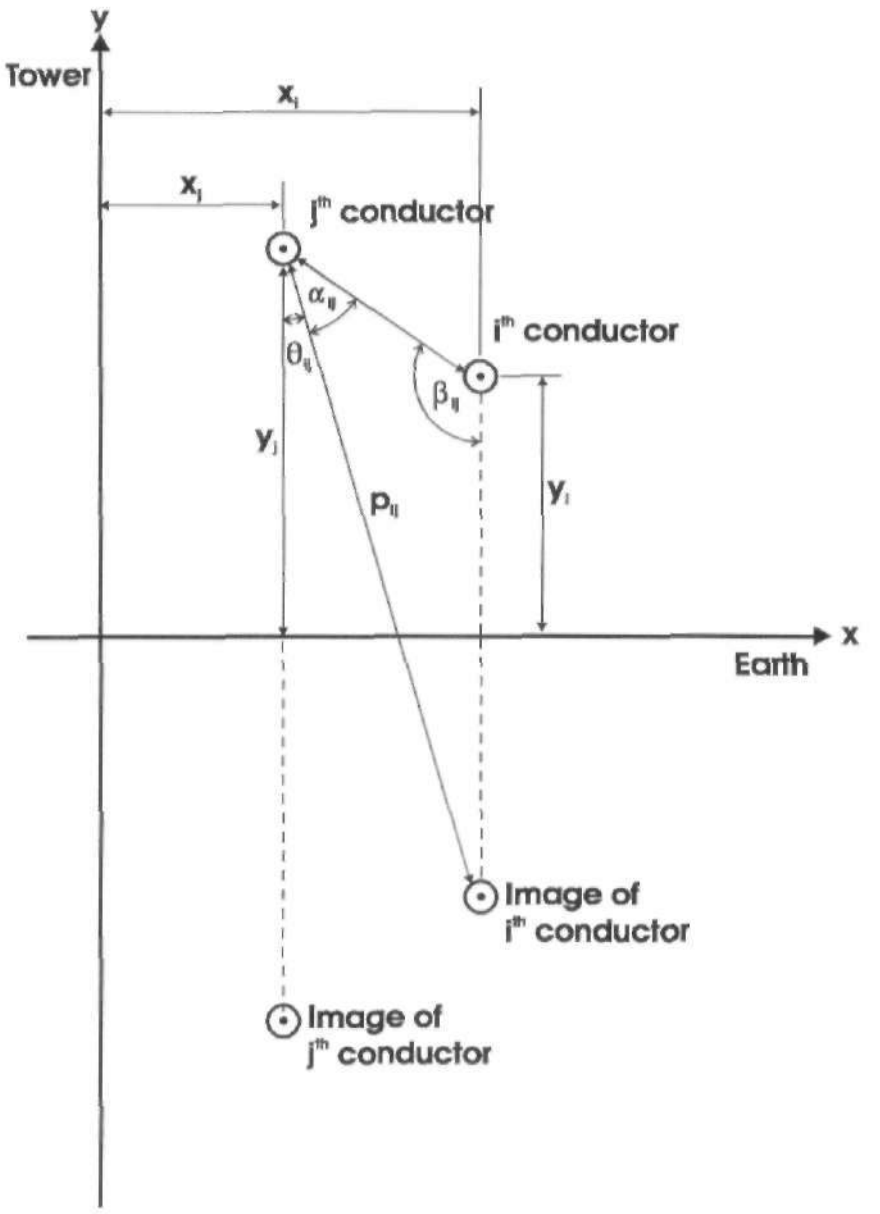



*Fig 2 8: Schematic of conductors*

$$D_{ij} = \sqrt{d_{ij}^{\,2} + 4y_i^2 - 4d_{ij}y_i \cos\beta_{ij}} \qquad (2\cdot3)$$

where, $\beta_{ij} = 180^\circ - (\alpha_{ij} + \theta_{ij})$ is the angle between the j[th] conductor and the image of the i[th] conductor and $\alpha_{ij} = \sin^{-1}\left(\frac{2y_i \sin\theta_{ij}}{d_{ij}}\right)$ is the angle between the i[th] conductors and its image.

It should be noted that the subscripts i and j are used for $\alpha$ to indicate the fact that its value depends on the position of conductors i and j. The order of matrix B is 3p+q where p is the number of circuits and q is the number of earth wires. Letting the charge matrix be $\Psi$ and voltage matrix, **V**, then,

$$\mathbf{V} = \left(\frac{1}{2\pi\varepsilon}\right)\mathbf{B}\Psi \qquad (2\cdot4)$$

where , $\varepsilon$ is the conductor permittivity. Thus, from equation (2.4),

$$\Psi = 2\pi\varepsilon\mathbf{B}^{-1}\mathbf{V} \qquad (2\cdot5)$$

Note that V is a column matrix whose last q elements are zero. This is because the earth wire voltage is zero and since the q rows of the $\mathbf{B}^{-1}$ matrix corresponds to the earth wire charges, they are removed from the matrix. The matrix $\mathbf{B}_A^{-1}$, which is obtained by discarding the last q rows and columns of $\mathbf{B}^{-1}$ is of order 3p [9].

The shunt admittance matrix, **Y** is defined by the equation:

$$\mathbf{I} = \mathbf{VY} \qquad (2\cdot6)$$

where ,

$$\mathbf{I} = \frac{d\Psi}{dt} = j\omega\Psi = j2\pi\omega\varepsilon\mathbf{B}_A^{-1}\mathbf{V} \qquad (2\cdot7)$$

and

$$\mathbf{Y} = j2\pi\omega\varepsilon\mathbf{B}_A^{-1} \qquad (2\cdot8)$$

where **Y** includes the effect of earth wires.

### 2-4-2 Calculation of the Impedance Matrix

The impedance matrix **Z′** has five components and is defined as follows:

$$\mathbf{Z}' = \mathbf{R}_c + \mathbf{R}_e + j\left(\mathbf{X}_g + \mathbf{X}_c + \mathbf{X}_e\right) \qquad (2\cdot9)$$

where $\mathbf{X}_g$ is the reactance due to physical geometry; $\mathbf{X}_c$, $\mathbf{R}_c$ are the reactance, resistance due to conductors; and $\mathbf{X}_e$, $\mathbf{R}_e$ are the reactance, resistance due to the effect of the earth-return path.

The order of matrix Z′ is 3p+q where, p is the number of circuits and q, the number of earth wires.

### 2·4·3 Reactance due to Physical Geometry

This reactance, $\mathbf{X}_g$ is calculated from [9]:

$$\mathbf{X}_g = \frac{\mu\omega\mathbf{B}}{2\pi} \qquad (2\cdot10)$$

where μ is the permeability of free space and **B** is as defined in equation (2.1).

### 2·4·4 Effect of Earth-Return Path

The contribution of resistance, $\mathbf{R}_e$ and reactance, $\mathbf{X}_e$, due to the earth-return path, is calculated by using the infinite series developed by Carson [12]. The real and imaginary correction component matrices $\mathbf{P}_e$ and $\mathbf{Q}_e$, respectively, can be expressed in terms of parameters r and θ, where,

$$r_{ij} = \sqrt{(\omega\mu/\rho)}D_{ij} \qquad (2\cdot11)$$

ρ is the earth resistivity and $\theta_{ij}$ is the angle subtended as shown in Fig. 2·8.

The elements of matrices $\mathbf{P}_e$ and $\mathbf{Q}_e$ can be determined as follows [12]:

For $r_{ij} \le 5$

$$P_{eij} = \frac{\pi}{8}(1-S_4) + \frac{1}{2}\log\left(\frac{2}{\gamma_{ij}}\right)S_2 + \frac{1}{2}\theta_{ij}S_2' - \frac{\sigma_1}{\sqrt{2}} + \frac{\sigma_2}{2} + \frac{\sigma_3}{\sqrt{2}} \qquad (2\cdot12)$$

$$Q_{eij} = \frac{1}{4} + \frac{1}{2}\log\left(\frac{2}{\gamma_{ij}}\right)(1-S_4) - \frac{1}{2}\theta_{ij}S_4' + \frac{\sigma_1}{\sqrt{2}} - \frac{\pi S_2}{8} + \frac{\sigma_3}{\sqrt{2}} - \frac{\sigma_4}{2} \qquad (2\cdot13)$$

For $r_{ij} > 5$

$$P_{eij} = \frac{\cos\theta_{ij}}{\sqrt{2}r_{ij}} - \frac{\cos 2\theta_{ij}}{r_{ij}^2} + \frac{\cos 3\theta_{ij}}{\sqrt{2}r_{ij}^3} + \frac{3\cos 5\theta_{ij}}{\sqrt{2}r_{ij}^5} \qquad (2\cdot14)$$

$$Q_{eij} = \frac{\cos\theta_{ij}}{\sqrt{2}r_{ij}} - \frac{\cos 3\theta_{ij}}{\sqrt{2}r_{ij}^3} + \frac{3\cos 5\theta_{ij}}{\sqrt{2}r_{ij}^5} \qquad (2\cdot15)$$

where $\gamma = 1.7811$ is the Euler's constant;

$$S_2 = \sum_0^\infty a_n \cos(4n+2)\theta_{ij}$$

$$S_2' = \sum_0^\infty a_n \sin(4n+2)\theta_{ij}$$

$$S_4 = \sum_0^\infty c_n \cos(4n+4)\theta_{ij}$$

$$S_4' = \sum_0^\infty c_n \sin(4n+4)\theta_{ij}$$

$$\sigma_1 = \sum_0^\infty e_n \cos(4n+1)\theta_{ij}$$

$$\sigma_2 = \sum_0^\infty g_n (S_2)_n$$

$$\sigma_3 = \sum_0^\infty f_n \cos(4n+3)\theta_{ij}$$

$$\sigma_4 = \sum_0^\infty h_n (S_4)_n$$

and

$$a_n = \frac{-a_{n-1}}{2n(2n+1)^2(2n+2)}\left(\frac{r_{ij}}{2}\right)^4; \quad a_0 = \frac{r_{ij}^2}{8}$$

$$c_n = \frac{-c_{n-1}}{(2n+1)(2n+2)^2(2n+3)}\left(\frac{r_{ij}}{2}\right)^4; \quad c_0 = \frac{r_{ij}^4}{192}$$

$$e_n = \frac{-e_{n-1}}{(4n-1)(4n-1)^2(4n+3)} r_{ij}^4; \quad e_0 = \frac{r_{ij}}{3}$$

$$f_n = \frac{-f_{n-1}}{(4n+1)(4n+3)^2(4n+5)} r_{ij}^4; \quad f_0 = \frac{r_{ij}^3}{45}$$

$$g_n = g_{n-1} + \frac{1}{4n} + \frac{1}{2n+1} + \frac{1}{2n+2} - \frac{1}{4n+4}; \quad g_0 = \frac{5}{4}$$

$$h_n = h_{n-1} + \frac{1}{4n+2} + \frac{1}{2n+2} + \frac{1}{2n+3} - \frac{1}{4n+6}; \quad h_0 = \frac{5}{3}$$

Therefore, the resistance and reactance due to the earth-return path will be given by:

$$R_{eij} = 2P_{eij}\mu\omega/2\pi \qquad (2\cdot16)$$

$$X_{eij} = 2Q_{eij}\mu\omega/2\pi \qquad (2\cdot17)$$

### 2·5 Components due to Conductors

At power frequency, it is assumed that $R_c$ equals the d.c. resistance per unit length of the

conductor. If skin effect is significant, however, the manufacturer's power frequency value is used.

At high frequencies, current is confined to the surface of the outer layer of the strands, due to skin effect. Assuming a small penetration depth, current density at the conductor surface is proportional to the magnetic field intensity at the surface. Under these conditions, the internal impedance is given by [13]:

$$Z_c = \frac{Km\rho}{r(n+2)\pi} \qquad (2\cdot18)$$

where, K = 2·25 is the conductor stranding factor; ρ is the conductor resistivity, r is the radius of each outer strand, n is the number of strands in the outer layer, and $m = \sqrt{(j\omega\mu/\rho)}$.

Thus,

$$R_c = X_c = \frac{Km\rho}{\sqrt{2}r(n+2)\pi} \qquad (2\cdot19)$$

### 2·4·6 Effect of Earth Wires in Impedance Matrix

Sections 2·4·3 through 2·4·6 allow the calculation of $\mathbf{Z}'$ as defined in equation (2.9). The equation relating the series voltage drop and current is:

$$\mathbf{V} = \mathbf{Z}'\mathbf{I} \Rightarrow \mathbf{I} = \mathbf{Z}'^{-1}\mathbf{V} \qquad (2\cdot20)$$

To determine the impedance matrix, **Z**, the last q rows and columns of $\mathbf{Z}'^{-1}$ are discarded for the same reasons given earlier in section 2·4·3. The resulting matrix $\mathbf{Z}^{-1}$ which is of order 3p is then inverted to obtain **Z**.

## 2·5 CALCULATION OF DERIVED PARAMETERS

The derived parameters are of two types:

(i) ***Electrically Short Lines*** - These are described in terms of symmetrical components assuming conductor symmetry;

(ii) ***Electrically Long Lines*** - These are described in terms of modal parameters.

### 2·5·1 Parameters for Electrically Short Lines

The matrix **Y**, which is an imaginary matrix and **Z** which is a complex matrix are required in the derivation of the power frequency symmetrical component parameters. The elements of **Z** provide

the series resistance and series reactance while the elements of **Y** provide the shunt-susceptance parameters. The parameters for the electrically short lines are $Z_1$, $Z_0$, $Z_{00}$, $Z_{PP}$, $Z_P$, $Z_{cc}$, $C_1$, $C_0$, $C_{00}$, $C_{PP}$, $C_P$ and $C_{cc}$. The calculation of these parameters takes the form of arithmetical operations on the elements as follows [10]:

$$Z_1 = \frac{1}{3}\left(Z_{11} + Z_{22} + Z_{33} - Z_{12} - Z_{13} - Z_{23}\right) \qquad (2\cdot21)$$

$$Z_0 = \frac{1}{3}\left(Z_{11} + Z_{22} + Z_{33} + 2Z_{12} + 2Z_{13} + 2Z_{23}\right) \qquad (2\cdot22)$$

$$Z_{00} = \frac{1}{3}\left(Z_{14} + Z_{15} + Z_{16} + Z_{24} + Z_{25} + Z_{26} + Z_{34} + Z_{35} + Z_{36}\right) \qquad (2\cdot23)$$

$$Z_{PP} = \frac{1}{3}\left(Z_0 - Z_1\right) \qquad (2\cdot24)$$

$$Z_P = Z_1 + Z_{PP} \qquad (2\cdot25)$$

$$Z_{cc} = \frac{1}{3}Z_{00} \qquad (2\cdot26)$$

For the shunt-susceptance parameters, let $\mathbf{A} = \mathbf{Y}^{-1}$ where **A** has elements $a_{ij}$.

Then,

$$C_1 = \frac{3}{\omega\left(a_{11} + a_{22} + a_{33} - a_{12} - a_{13} - a_{23}\right)} \qquad (2\cdot27)$$

$$C_0 = \frac{3}{\omega\left(a_{11} + a_{22} + a_{33} + 2a_{12} + 2a_{13} + 2a_{23}\right)} \qquad (2\cdot28)$$

$$C_{00} = \frac{3}{\omega\left(a_{14} + a_{15} + a_{16} + a_{24} + a_{25} + a_{26} + a_{34} + a_{35} + a_{36}\right)} \qquad (2\cdot29)$$

$$C_{PP} = \frac{3}{\frac{1}{C_0} - \frac{1}{C_1}} \qquad (2\cdot30)$$

$$C_P = \frac{1}{\frac{1}{C_1} - \frac{1}{C_{PP}}} \qquad (2\cdot31)$$

$$C_{cc} = 3C_{00} \qquad (2\cdot32)$$

The symbols are interpreted as follows:

$Z_1$ positive-sequence impedance;

$Z_0$ zero-sequence impedance;

$Z_{00}$ zero-sequence mutual impedance;

$Z_{PP}$ interphase mutual impedance;

$Z_P$ earth-loop impedance;

$Z_{cc}$ intercircuit mutual impedance;

$C_1$ positive-sequence capacitance;

$C_0$ zero-sequence capacitance;

$C_{00}$ zero-sequence mutual capacitance;

$C_{PP}$ interphase mutual capacitance;

$C_P$ earth-loop capacitance;

$C_{cc}$ intercircuit mutual capacitance.

Fig.2·9 and Fig.2·10 show the equivalent circuits relating to the series and shunt parameters. It should be noted that the parameters $Z_{00}$, $Z_{cc}$, $C_{00}$ and $C_{cc}$ only apply to 330 kV lines.

### 2·5·2 Parameters for Electrically Long Lines

The parameters for the electrically long lines are the characteristic impedance, the characteristic admittance, the mode propagation constants and the mode-distribution vectors. Here, the equations are solved in terms of travelling-wave modes [9] which can be described as follows:

For a particular frequency, each mode is associated with a certain voltage and current distribution in the conductors and a propagation coefficient. A characteristic impedance matrix and a characteristic admittance matrix is also obtained for that frequency. The solution is obtained using the root-squaring method by first evaluating the eigenvalues and eigenvectors of the complex matrix, **P**, formed from:

$$\mathbf{P} = \mathbf{ZY} \qquad (2 \cdot 33)$$

That is, the eigenvalues, $\lambda_i$ and the eigenvector matrix **Q** are found such that:

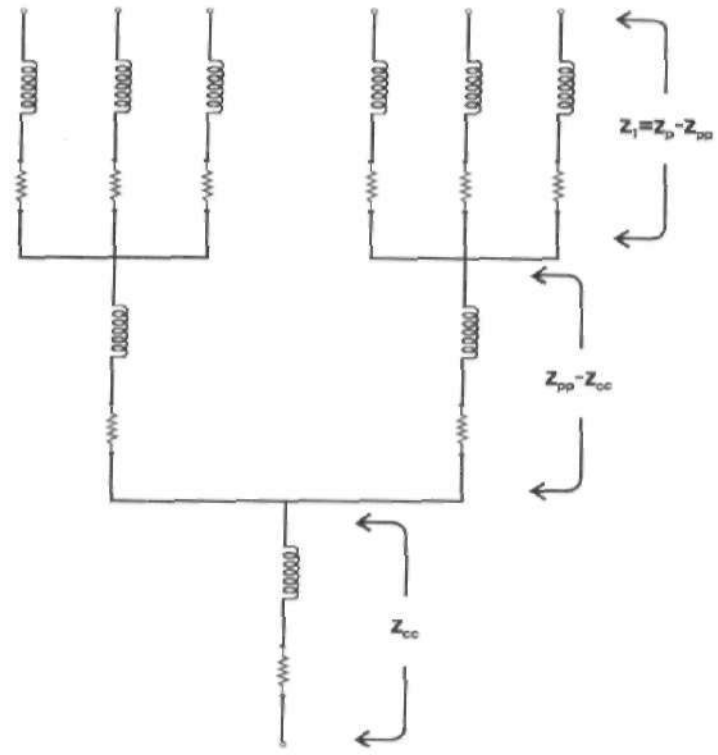



*Fig 2 9: Series symmetrical-component equivalent circuit for electrically short lines*

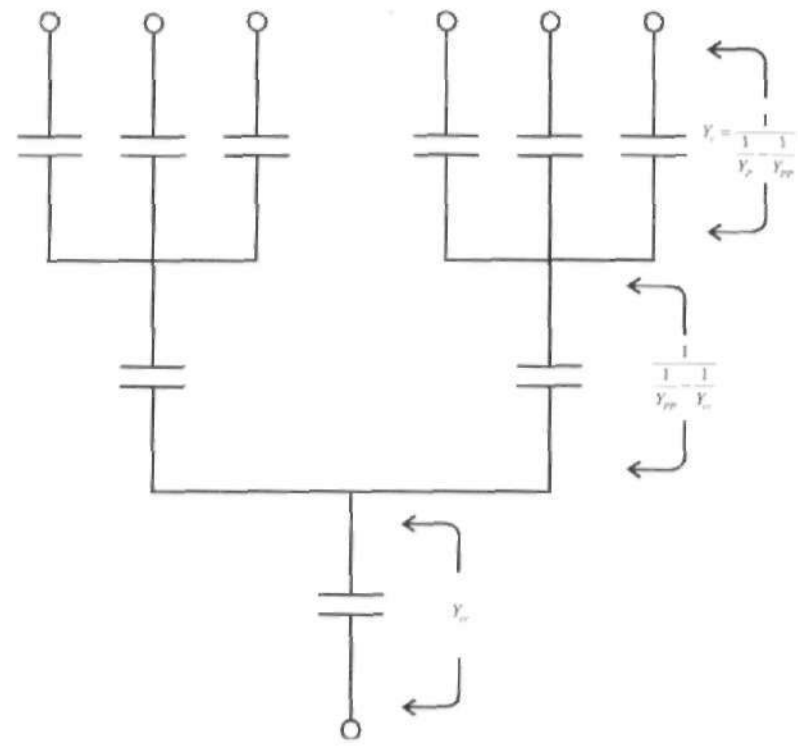


*Fig 2 10: Shunt symmetrical-component equivalent circuit for electrically short lines*

$$|\mathbf{P} - \mathbf{i}\lambda_i| = 0 \qquad (2\cdot34)$$

$$\mathbf{QPQ}^{-1} = diag[\lambda_i] \qquad (2\cdot35)$$

The columns of **Q**, which are the eigenvectors of **P**, give the mode distributions of voltage corresponding to the values $\lambda_i$.

The mode distributions of current are determined from:

$$\mathbf{S} = \left[\mathbf{Q}^{\mathrm{T}}\right]^{-1} \qquad (2\cdot36)$$

where, T denotes matrix transpose.

Propagation constant of mode i is given by:

$$\gamma_i = \sqrt{\lambda_i}\,(\equiv \alpha_i + j\beta_i) \qquad (2\cdot37)$$

where, $\alpha_i$ and $\beta_i$ are the attenuation and phase of mode i respectively. Also, velocity factor is given by:

$$\mu_i = \omega/\beta_i \qquad (2\cdot38)$$

where, $\omega$ is the angular frequency.

The characteristic-impedance matrix $\mathbf{Z}_0$ is:

$$\mathbf{Z}_0 = \mathbf{Q}\gamma^{-1}\mathbf{Q}^{-1}\mathbf{Z} \qquad (2\cdot39)$$

and the characteristic-admittance matrix $\mathbf{Y}_0$ is:

$$\mathbf{Y}_0 = \mathbf{Z}\mathbf{Q}\gamma^{-1}\mathbf{Q}^{-1} \qquad (2\cdot40)$$

In order to consider a symmetrical twin-circuit line with a vertical axis of symmetry, **Z** and **Y** will have to be factorized before the eigenvectors and eigenvalues are found [9].

This chapter has considered the requirements for the calculation of the basic impedance and admittance matrices per unit length as well as the symmetrical component parameters and the modal parameters. In the next chapter, the data collected from NEPA is analysed by using digital computer programs.

# CHAPTER THREE

## COMPUTER-AIDED DATA ANALYSIS

### 3·1 INTRODUCTION

The use of a digital computer to aid in the analysis of carrier propagation on the 132kV transmission lines became necessary because of the complexity of the mathematical expressions involved. The SKV model computer machine which was used for this analysis has the following features:

GD5320 VGA ROM BIOS Version 3·08

| | |
|---|---|
| Main processor | : 80386 |
| Numeric processor | : None |
| Floppy drive A | : 1.44MB, 3·5" |
| Floppy drive B | : None |
| Display | : VGA/PGA/EGA |
| ROM BIOS date | : 04/30/91 |
| Base memory size | : 640kB |
| Extended memory size | : 1024kB |
| Hard disk C | : Type 47 |
| Hard disk D | : None |
| Serial ports | : 3F8, 2F8 |
| Parallel ports | : 378 |
| Operating system | : Disk Operating System (DOS), version 6·21 |

The 132kV circuits of the National Electric Power Authority are divided into regions, one of which is the Kaduna Region (see Appendix F). The Shiroro Complex of the Kaduna region is taken for analysis because it is the most newly commissioned circuit and, for this reason, one expects the lines in that complex to exhibit true propagation characteristics given accurate data or parameter specifications. The location of the Shiroro complex is shown in Appendix E. Table 3·1 shows the line impedances for Kaduna Region 132kV circuits as obtained from NEPA, and out of these, the following lines constitute the Shiroro Complex.

*Table 3·1: Line impedances for Kaduna Region 132 kV circuits (See Appendix A)*

| Line Name | Type | Line Length (KM) | Positive Sequence Impedance (Ohms) | Zero Sequence Impedance (Ohms) |
|---|---|---|---|---|
| Kaduna-Kaduna Town | DC-WOLF | 13 | 5·95/63° | 18·49/74° |
| Kaduna-Zaria | SC-WOLF | 72 | 33·26/63° | 115·90/74° |
| Zaria-Sokoto | SC-WOLF | 363 | 167·00/63° | 584·51/74° |
| Zaria-Kano | SC-WOLF | 145 | 66·99/63° | 233·48/74° |
| Kano-Dankata | DC-WOLF | 12 | 5·50/63° | 17·07/74° |
| Kano-Katsina | DC-WOLF | 180 | 82·35/63° | 255·98/74° |
| Kano-Dan Agundi | SC-WOLF | 8 | 3·70/63° | 12·88/74° |
| Dankata-Hadejia | SC-WOLF | 150 | 64·35/63° | 241·53/74° |
| Jos-Bauchi | SC-WOLF | 118 | 54·50/63° | 190·00/74° |
| Bauchi-Gombe | SC-WOLF | 146 | 67·45/63° | 235·10/74° |
| Gombe-Yola | SC-WOLF | 216 | 99·79/63° | 347·80/74° |
| Gombe-Biu | SC-WOLF | 126 | 58·21/63° | 202·89/74° |
| Gombe-Potiskum | SC-WOLF | 181 | 83·61/63° | 291·48/74° |
| Biu-Maiduguri | SC-WOLF | 177 | 80·38/63° | 285·00/74° |
| Shiroro-Minna | DC-WOLF | 53 | 24·25/63° | 75·37/74° |
| Shiroro-Tegina | SC-WOLF | 65 | 30·03/63° | 104·66/74° |
| Tegina-Kontagora | SC-WOLF | 100 | 46·20/63° | 161·02/74° |
| Kontagora-Yelwa | SC-WOLF | 109 | 50·36/63° | 175·51/74° |
| Minna-Bida | SC-WOLF | 90 | 41·58/63° | 144·92/74° |
| Minna-Abuja | DC-WOLF | 136 | 62·22/63° | 193·41/74° |

*Table 3.2: Line parameters for Shiroro Complex 132 kV lines (See Appendix B)*

| S/No | PARAMETER | SPECIFICATION |
|---|---|---|
| 1 | Positive-sequence impedance, $Z_1$ | 0·1937 + j 0·4139 Ω/km |
| 2 | Negative-sequence impedance, $Z_2$ | 0·1937 + j 0·4139 Ω/km |
| 3 | Zero-sequence impedance, $Z_0$ | 0·3863 + j 1·3648 Ω/km |
| 4 | Mutual capacitance, G | $1·12 \times 10^{-9}$ F/km |
| 5 | Operating capacitance, $C_1$ | $8·82 \times 10^{-9}$ F/km |
| 6 | Capacitance-to-earth, $C_0$ | $5·45 \times 10^{-9}$ F/km |
| 7 | Surge impedance, Z | 386·47 Ω |
| 8 | Surge capacity, $P_W$ | 45·08 MW |
| 9 | Charging capacity, $P_L$ | 0·0483 MVAR/km |
| 10 | Charging current, $I_L$ | 0·211 A/km |
| 11 | Earth-leakage current, $I_E$ | 0·391 A/km |
| 12 | Maximum boundary field strength, L | 13·3kV |
| 13 | Conductor type | ACSR (WOLF) |
| 14 | Conductor size, CSA | 194·4 $mm^2$ |
| 15 | Load current, $I_{LI}$ | 178 A |
| 16 | Load current, $I_{LII}$ | 178 A |
| 17 | Load current, $I_{LIII}$ | Not available |
| 18 | Load current, $I_{LIV}$ | 40 A |
| 19 | Weight of conductor | 726 kg/km |
| 20 | Protecting treatment | Steel core greased |
| 21 | Earth wire type | Steel |
| 22 | Earth wire size, CSA | 38·6 $mm^2$ |
| 23 | Shielding/shielding angle | Single earth wire 30° |
| 24 | Maximum wind span | 390 m |
| 25 | Design span | 350 m (up to 400 m okay) |
| 26 | Maximum weight span | T10 m |
| 27 | Height of tower | 24·2 m (SS2L) - 42·4 m(SSWL) |
| 28 | Body extension | +0 to +9 m |
| 29 | Voltage level | 132 kV |

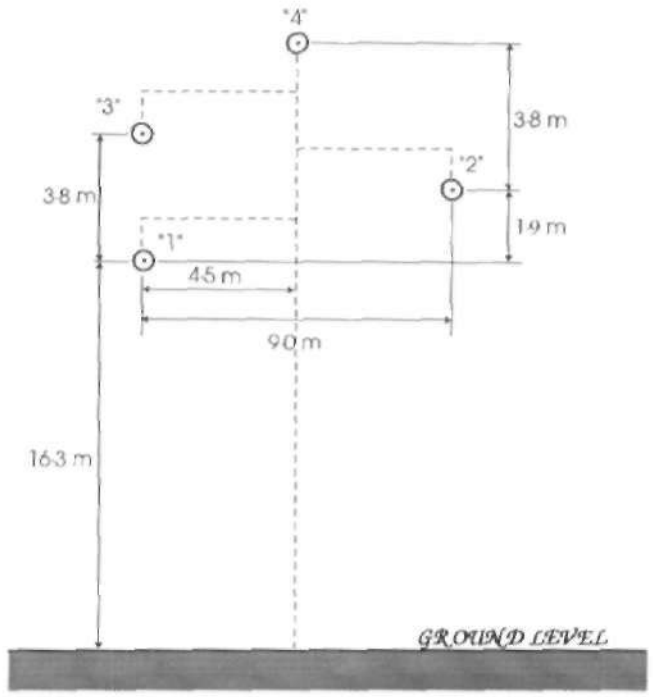



***Fig 3-1: Configuration of Shiroro Complex 132 kV line (See Appendix C)***

1) Minna-Suleja-Abuja Line I (Load Current, $I_{LI}$ = 178A)

2) Minna-Suleja-Abuja Line II (Load Current, $I_{LII}$ = 178A)

3) Minna-Bida Line (Load Current, $I_{LIII}$ is not available)

4) Shiroro-Tegina Line (Load Current, $I_{LIV}$ = 40A).

The load current for the Minna-Bida Line is left blank because the value was not supplied by NEPA.

## 3.2 DATA

The method of analysis discussed in Chapter Two was applied to NEPA 132kV lines, Shiroro complex. The line configuration is shown in Fig. 3-1 and the line constants as obtained from NEPA are presented in Table 3-2. Although, load currents no doubt have some effects on the attenuation, they were not taken into consideration in this project. Perhaps in subsequent works, these effects can be investigated.

The value of some parameters were based on assumption. For example, the earth resistivity, $\rho_e$, was taken as 100 $\Omega$ m and the relative permeability, $\mu_r$, was taken as $10^3$. Also, since the resistivity of Aluminium is $3.21 \times 10^{-8}\ \Omega$ m and we have the Aluminium Steel Reinforced Concrete conductor, the

mean resistivity calculated as $3{\cdot}82 \times 10^{-8}\,\Omega$ m was used as the conductor resistivity.

### 3·2·1 Determination of Input Data for High Frequency Calculations( HFC)

From Table 3·2 obtained from NEPA, input data were derived for the calculation of high frequency parameters as shown in the next two sections.

### 3·2·2 Determination of Conductor Input Parameters for HFC

#### *Resistivity*

If $\rho_s$ and $\rho_A$ represent the resistivity of steel and aluminium, respectively, then the mean resistivity of the conductor will be given by:

$$\rho_c = \frac{\rho_s \rho_A}{\rho_s - \rho_A} \qquad (3{\cdot}1)$$

where, $\rho_s = 20{\cdot}0 \times 10^{-8}\,\Omega$ m

$\rho_A = 3{\cdot}21 \times 10^{-8}\,\Omega$ m.

#### *Radius*

The conductor radius is given by:

$$r_c = \left(\frac{CSAC}{\pi}\right)^{1/2} \qquad (3{\cdot}2)$$

where, CSAC is the conductor cross- sectional area.

#### *Radius of each strand*

Since the conductor is made up of aluminium and steel, the conductor cross-sectional area is the algebraic sum of the cross-sectional areas of aluminium and steel. If CSAA and CSAS denote the cross-sectional area of aluminium and steel, respectively with $N_A$ and $N_s$ number of strands, then the radius of each strand of aluminium, $r_A$ and that of steel, $r_s$ will be given by:

$$r_A = \left(\frac{CSAA}{\pi N_A}\right)^{1/2} \qquad (3{\cdot}3)$$

$$r_s = \left(\frac{CSAS}{\pi N_s}\right)^{1/2} \qquad (3{\cdot}4)$$

### 3·2·3 Determination of Earth Wire Input Parameters for HFC

#### *Resistivity*

Since the earth wire is made up of steel, the resistivity simply corresponds to the value of $\rho_s$ given in equation 3·1.

#### *Radius*

The radius of the earth wire, $r_e$, is given by:

$$r_e = \left(\frac{CSAE}{\pi}\right)^{1/2} \qquad (3\cdot5)$$

KASHIM IBRAHIM LIBRARY
23 AUG
ZARIA NIGERIA
Ahmadu Bello University

where, CSAE is the earth wire cross-sectional area.

### 3·2·4 Determination of Input Data for Power Frequency Calculations( PFC)

Here, the physical layout of the line and the parameters $r_c$, $r_A$, $r_s$ and $r_e$ would be used.

### 3·2·5 Determination of Conductor Input Parameter for PFC

#### *Coordinates*

The coordinates are obtained directly from Fig. 3·1. The dimensions are in metres(m). Each position stated in the figure represents a mode. Mode distribution refers to an injection between a conductor to ground with the remaining conductors grounded. For example, when the injection is between conductor 2 to ground, the mode is referred to as mode 2 distribution.

Therefore, the coordinates of the conductors in each mode are:

Mode 1 : (-4·5, 20·1)

Mode 2 : (4·5, 18·2)

Mode 3 : (-4·5, 16·3).

It should be noted that the mode distribution does not apply to the earth wire.

#### *Resistance per unit length*

Generally, the resistance, $R_m$, of a material is given by:

$$R_m = \rho\frac{l}{A} \Rightarrow R = \frac{R_m}{l} = \frac{\rho}{A} \qquad (3\cdot6)$$

where, $\rho$ is the resistivity of the material, $l$ is the length of the material, and A is the cross-sectional

area (CSA) of the material. R is the resistance per unit length of the material.

Therefore $R_c$, the conductor resistance per unit length is given by:

$$R_c = \frac{\rho_c}{CSAC} \qquad (3\cdot7)$$

where, $\rho_c$ and CSAC are as given in equations (3.1) and (3.2).

### 3·2·6 Determination of Earth Wire Input Parameters for PFC

#### *Coordinates*

The coordinates are obtained directly from Fig. 3·1. The dimensions are in metres. Since the earth wire is shown in position 4 of the figure, the coordinate is given by:

position 4 : (0·0, 22·0)

#### *Resistance per unit length*

The earth wire resistance per unit length, $R_e$, is given by:

$$R_e = \frac{\rho_s}{CSAE} \qquad (3\cdot8)$$

where, $\rho_s$ is the resistivity of earth wire, and CSAE is the cross-sectional area of the earth wire.

## 3·3 INPUT DATA FOR HFC

The data supplied by NEPA (see Appendix B) are listed as follows:

CSAC = 194·9 mm$^2$

CSAA = 150·0 mm$^2$

CSAS = 44·9 mm$^2$

$N_A$ = 30

$N_s$ = 7

CSAE = 38·6 mm$^2$

Using equations (3.1) through (3.5), the input data was obtained for high frequency calculations as outlined in the next two sections.

### 3·3·1 Conductor Input Data for HFC

Conductor mean resistivity, $\rho_c = 3{\cdot}82 \times 10^{-8}\ \Omega\,m$

Conductor radius, $r_c = 7{\cdot}88$ mm

Radius of one Aluminium strand, $r_A = 1{\cdot}262$ mm

Radius of one Steel strand, $r_s = 1{\cdot}429$ mm.

### 3·3·2 Earth Wire Input Data for HFC

Earth Wire resistivity, $\rho_s = 20{\cdot}0 \times 10^{-8}\,\Omega\,m$

Earth radius, $r_e = 3{\cdot}505$ mm

Earth resistivity, $\rho_e = 100{\cdot}0\,\Omega\,m$

Relative permeability, $\mu_r = 1000{\cdot}0$.

## 3·4 INPUT DATA FOR PFC

The conductors geometry supplied by NEPA are listed as follows:

Position 1 : (-4·5, 20·1)

Position 2 : (4·5, 18·2)

Position 3 : (-4·5, 16·3)

Position 4 : (0·0, 22·0).

Using equations (3.7) and (3.8), the input data was obtained for power frequency calculations as follows:

Conductor resistance, $R_c = 0{\cdot}1554\,\Omega/km$

Earth wire resistance, $R_e = 5{\cdot}181\,\Omega/km$

## 3·5 PROGRAM AND RESULTS

The use of digital computer is necessary to reduce the rigours of the mathematical expressions involved in multiconductor-line problems. For this reason, the mathematical equations presented in Chapter Three were used to develop a software applications program.

### 3·5·1 The Program

The modular approach to programming was used in this project instead of the block approach. Programming which uses the modular approach is called structured programming. In the modular approach, the program consists of a short main program and a series of subprograms or subroutines, all linked to modules. The sequence of calling of these subroutines determines the sequence of proce-

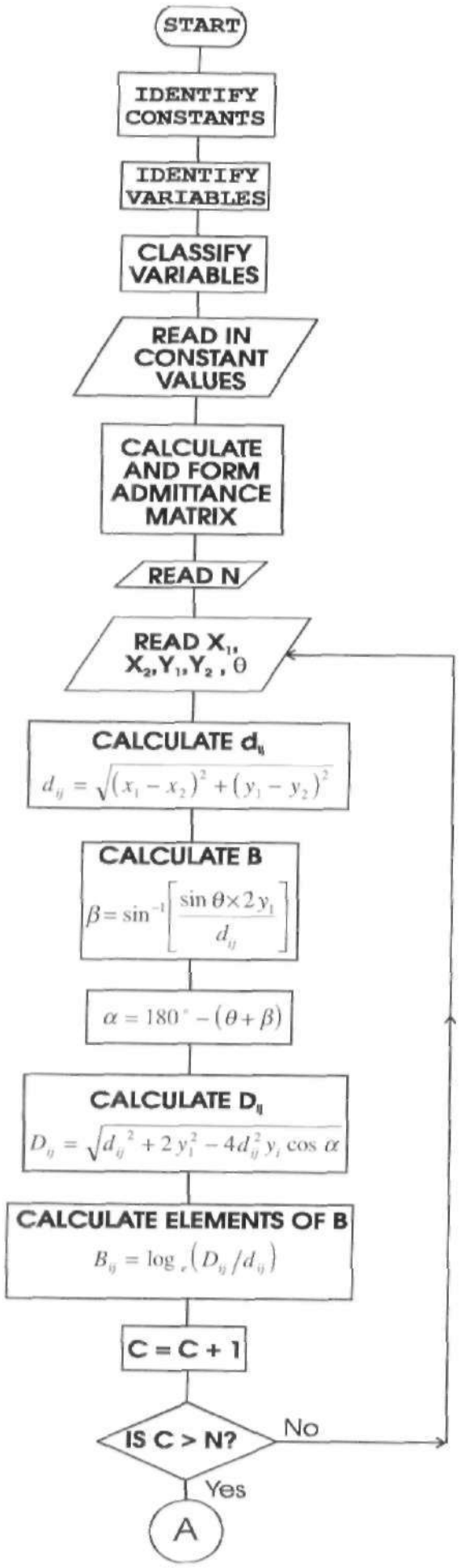



*Fig 3.2: Flow chart representation of the block program*

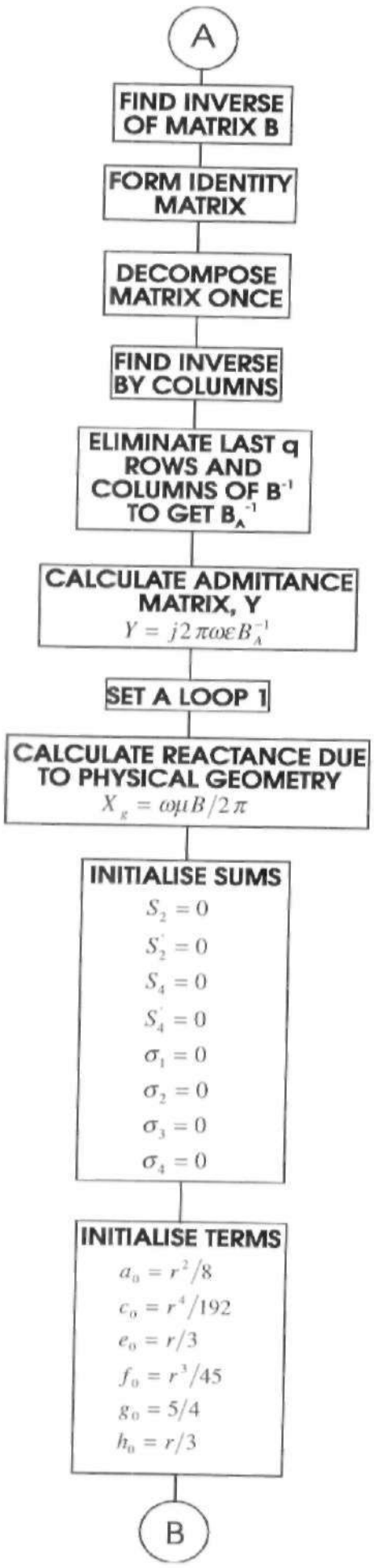



*Fig 3.2 (Continued): Flow chart representation of the block program*

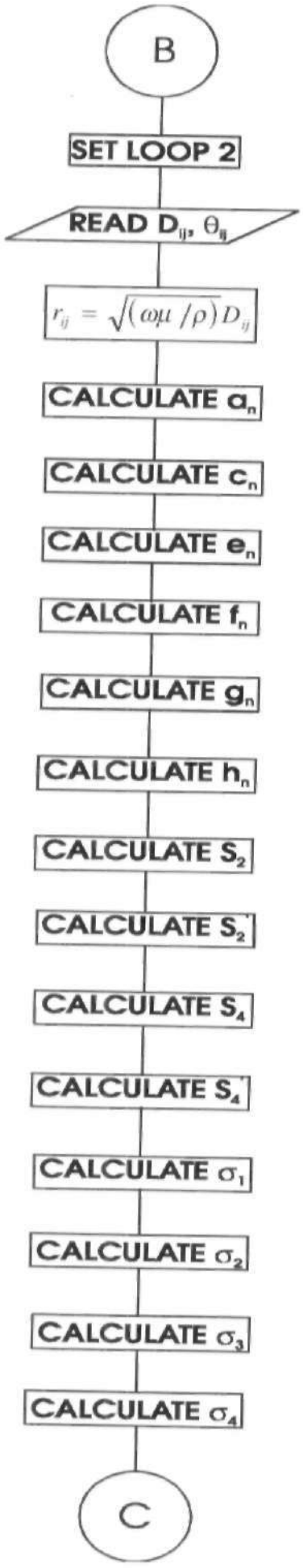



*Fig 3.2 (Continued): Flow chart representation of the block program*

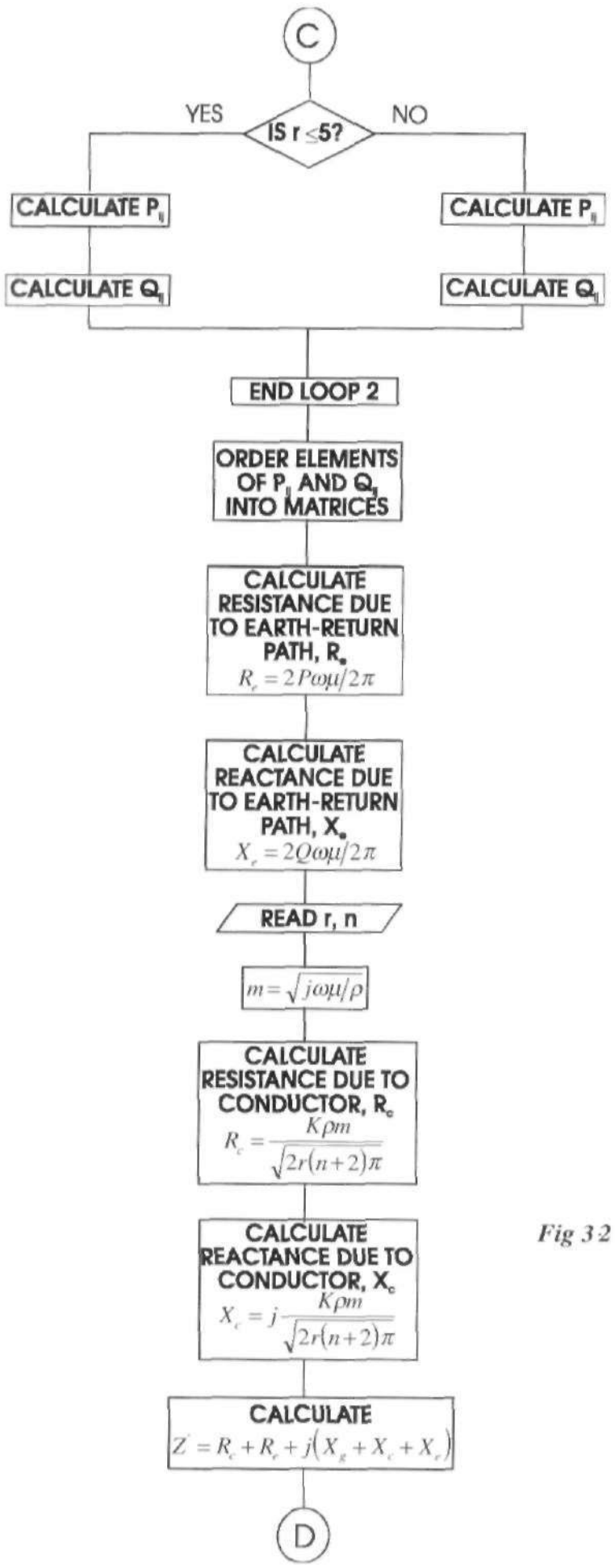



*Fig 3.2 (Continued): Flow chart representation of the block program*

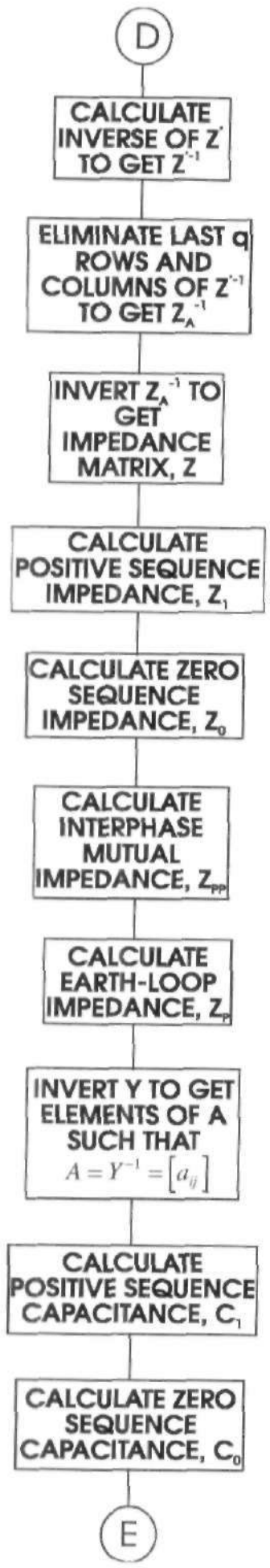



*Fig 3.2 (Continued): Flow chart representation of the block program*

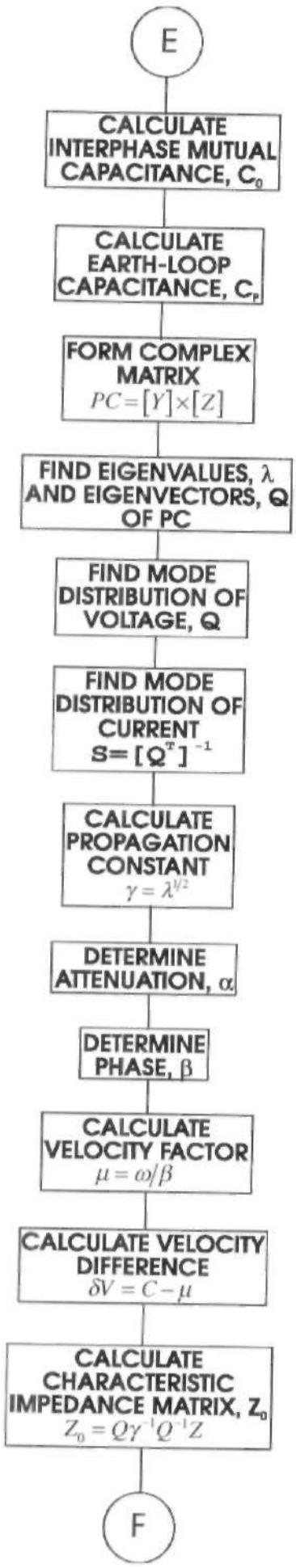



*Fig 3.2 (Continued): Flow chart representation of the block program*

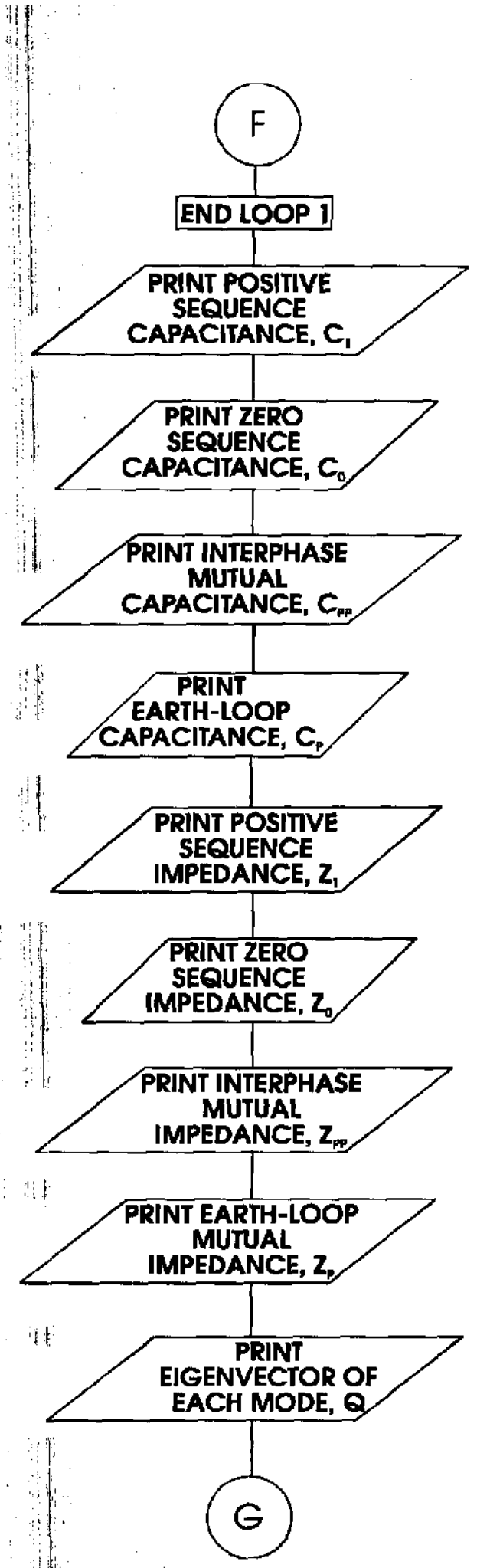



*Fig 3 2 (Continued): Flow chart representation of the block program*

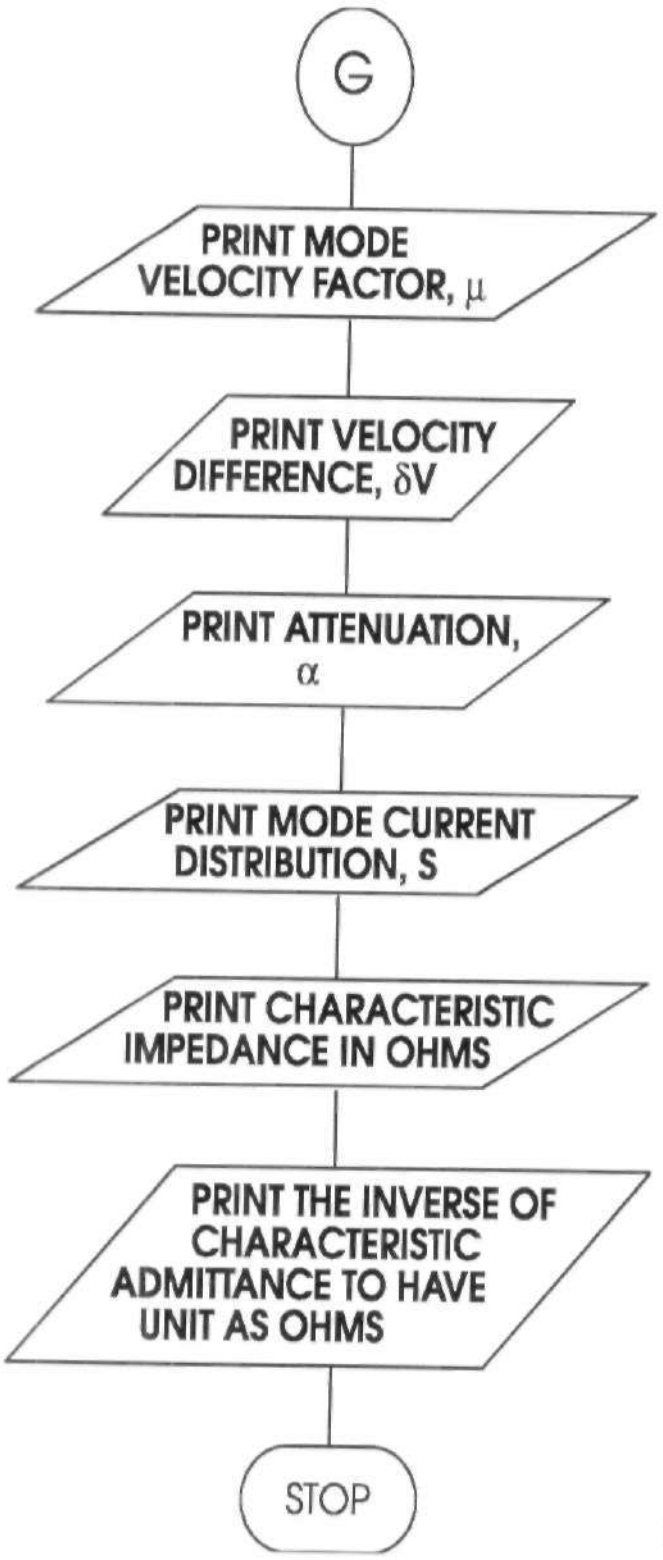



*Fig 3.2 (Continued): Flow chart representation of the block program*

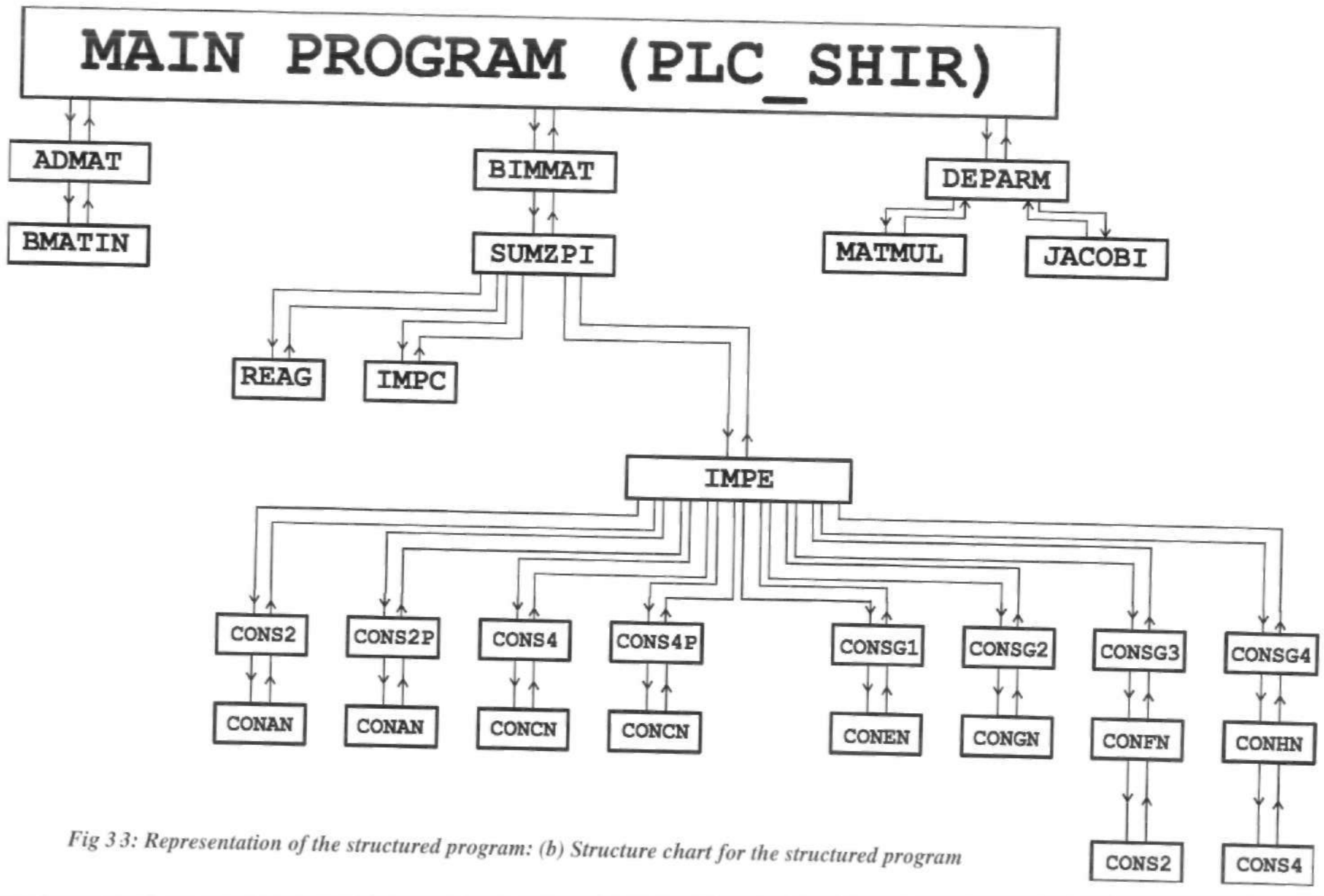



*Fig 3.3: Representation of the structured program: (b) Structure chart for the structured program*

dure, and ideally, everything passed through the main program would be an input and output parameter only. All modules are as *GO TO-less* as possible.

Structured programming was used in this project because structured programs are easier to read, easier to maintain, easier to modify, easier to test and debug and easier to learn. Although structured programs, compared to block programs, have the disadvantages of consuming more core space, more central processing unit time of compilation and execution, more design time from programmer and more lines of code, they are preferred to block programs by many programmers because of the advantages mentioned earlier.

Although the block program was not used in this project, it became necessary to present a schematic visual description of the logic of the block program module for greater coverage. This is shown in Fig. 3·2. Also, the structured program used for this project may be represented by its structure chart and its main block shown in Fig. 3·3. The structured program identified as **PLC_SHIR** (see APPENDIX D) has been developed to conform to American National Standards Institute, ANSI FORTRAN 77. Thus, the program is very portable.

### 3·5·2 Analysis of Results

The results have been divided into two groups, namely, those involving parameters obtained at power frequency and those involving parameters at higher frequencies.

Tables 3·3 through 3·6, Fig. 3·4 and Fig. 3·5 describe the propagation characteristics of the Shiroro Complex 132kV powerline carrier signals.

In this project, there are three mode distribution vectors comprising mode 1, mode 2 and mode 3 which are associated with conductor 1, conductor 2 and conductor 3, respectively. In Fig. 3·5, the differences between the free space velocity and the mode propagation velocities are plotted for clarity since as can be observed, the mode propagation velocities obtained are very close to the free space velocity value, $3 \times 10^5$ kms$^{-1}$.

An interesting example is the situation shown in Table 3·5 where the attenuation of mode 1 at a frequency of 100kHz is 0·82 dB/km. This is much higher than that of mode 2 which is 0·0748 dB/km which means that at the receiving end, the only significant power is that contained in mode 2. The power contained in mode 1 is much rapidly attenuated so that, relative to the total power, it is equiva-

lent to a fixed insertion loss, independent of the line length. Therefore, the line attenuation for this condition of energization requires mode 2 consideration only, having determined the insertion loss due to mode 1.

Table 3·6 presents a situation which is similar to that shown in Table 3·5. Although the signal attenuation on the line is high in modes 2 and 3, these modes still contain little power at the receiving end compared to that in mode 1. One could see from this table that signal attenuation at 1MHz is so high that one gets little or no power at the receiving end.

Table 3·7 shows the calculated parameters for the power frequency. The consideration of the effect of the earth-return path in the calculations as given in section 2·4·4 provide a higher level of accuracy.

Fig. 3·6 shows the variation of attenuation with velocity difference. From this figure, it can be observed that mode 2 provides an approximately linear characteristic. By drawing a tangent to point (45000,0·36), mode 1 was found to be linear between points (87500,0·0072) and (45000,0·36). For mode 3, a region exists for which there is inflexion. This region is bounded between points (4250,0·02) and (7500,0·096). The point of inflexion is about (6000,0·018) and is the point at which the curves for mode 2 and mode 3 intersect.

It should be noted that the attenuation characteristics obtained were based on an average data collected from NEPA for the Shiroro Complex taken as a whole and not on the four individual lines in the complex. It is possible however, to consider the individual lines, in which case, the attenuation characteristics will have to be studied for the individual load capacities of the lines. This could be considered as a further study.

*Table 3.3: Derived parameters for electrically long lines at 1 kHz frequency*

Characteristic impedance, $Z_0$ ($\Omega$)

$$Z_0 = \begin{bmatrix} 509 - j9 & 82 - j6 & 141 - j8 \\ 82 - j6 & 494 - j8 & 92 - j6 \\ 141 - j8 & 92 - j6 & 482 - j6 \end{bmatrix}$$

Characteristic admittance, $Y_0$ ($\Omega$)

$$Y_0 = \begin{bmatrix} 395 - j5 & -3045 - j154 & -1889 - j43 \\ -3045 - j154 & 381 - j3 & -2002 - j68 \\ -1889 - j43 & -2002 - j68 & 298 - j2 \end{bmatrix}$$

Propagation constants

Mode 1

| $\alpha$ | $\beta$ | $\mu$ | $\delta V$ |
|---|---|---|---|
| 0·01 | 0·0296 | 212000 | 82000 |

Mode 2

| $\alpha$ | $\beta$ | $\mu$ | $\delta V$ |
|---|---|---|---|
| 0·00748 | 0·0216 | 290720 | 9280 |

Mode 3

| $\alpha$ | $\beta$ | $\mu$ | $\delta V$ |
|---|---|---|---|
| 0·00712 | 0·0216 | 290360 | 9640 |

Mode-distribution vectors

Voltage

| Mode 1 | Mode 2 | Mode 3 |
|---|---|---|
| 0·221 – j0·002 | 0·053 – j0·073 | –0·342 – j0.005 |
| 0·209 – j0·004 | –0·101 – j0·012 | –0·097 – j0.016 |
| 0·198 – j0·004 | 0·021 + j0·004 | –0·706 + j0.000 |

Current

| Mode 1 | Mode 2 | Mode 3 |
|---|---|---|
| 1·178 + j0·041 | 3·342 – j0·470 | –0·572 – j0·009 |
| 1·121 + j0·013 | –4·314 + j0·451 | –0·190 + j0·022 |
| 1·000 + j0·000 | 1·000 + j0·000 | 1·000 + j0·000 |

***Table 3 5: Derived parameters for electrically long lines at 100 kHz frequency***

Characteristic impedance, $Z_0(\Omega)$

$$Z_0 = \begin{bmatrix} 435 - j7 & 68 - j5 & 102 - j6 \\ 68 - j5 & 432 - j7 & 79 - j5 \\ 102 - j6 & 79 - j5 & 428 - j6 \end{bmatrix}$$

Characteristic admittance, $Y_0(\Omega)$

$$Y_0 = \begin{bmatrix} 398 - j4 & -3112 - j154 & -2009 - j45 \\ -3112 - j154 & 384 - j3 & -2264 - j73 \\ -2009 - j45 & -2264 - j73 & 356 - j3 \end{bmatrix}$$

Propagation constants

Mode 1

| $\alpha$ | $\beta$ | $\mu$ | $\delta V$ |
|---|---|---|---|
| 0·82 | 2·3413 | 268400 | 31600 |

Mode 2

| $\alpha$ | $\beta$ | $\mu$ | $\delta V$ |
|---|---|---|---|
| 0·0748 | 2·1080 | 298100 | 1900 |

Mode 3

| $\alpha$ | $\beta$ | $\mu$ | $\delta V$ |
|---|---|---|---|
| 0·0712 | 2·1012 | 299072 | 928 |

Mode-distribution vectors

Voltage

| Mode 1 | Mode 2 | Mode 3 |
|---|---|---|
| 0·272– *j*0·002 | 0·083– *j*0·115 | –0·379– *j*0·006 |
| 0·234– *j*0·005 | –0·120– *j*0·014 | –0·124+ *j*0·020 |
| 0·226– *j*0·005 | 0·025+ *j*0·005 | 0·736+ *j*0·000 |

Current

| Mode 1 | Mode 2 | Mode 3 |
|---|---|---|
| 1·259+ *j*0·037 | 3·479– *j*0·481 | –0·559– *j*0·010 |
| 1·176+ *j*0·013 | –4·788+ *j*0·497 | –0·203+ *j*0·022 |
| 1·000+ *j*0·000 | 1·000+ *j*0·000 | 1·000+ *j*0·000 |

*Table 3 6: Derived parameters for electrically long lines at 1MHz frequency*

Characteristic impedance, $Z_0(\Omega)$

$$Z_0 = \begin{bmatrix} 413 - j7 & 62 - j4 & 95 - j5 \\ 62 - j4 & 405 - j6 & 67 - j4 \\ 95 - j5 & 67 - j4 & 398 - j5 \end{bmatrix}$$

Characteristic admittance, $Y_0(\Omega)$

$$Y_0 = \begin{bmatrix} 426 - j5 & -3098 - j145 & -1987 - j43 \\ -3098 - j145 & 413 - j4 & -2018 - j65 \\ -1987 - j43 & -2818 - j65 & 397 - j3 \end{bmatrix}$$

Propagation constants

Mode 1

| $\alpha$ | $\beta$ | $\mu$ | $\delta V$ |
|---|---|---|---|
| 6·04 | 21·535 | 291800 | 8200 |

Mode 2

| $\alpha$ | $\beta$ | $\mu$ | $\delta V$ |
|---|---|---|---|
| 0·496 | 20·991 | 299360 | 640 |

Mode 3

| $\alpha$ | $\beta$ | $\mu$ | $\delta V$ |
|---|---|---|---|
| 0·3772 | 20·984 | 299468 | 532 |

Mode-distribution vectors

Voltage

| Mode 1 | Mode 2 | Mode 3 |
|---|---|---|
| 0·296– *j*0·002 | 0·103– *j*0·132 | –0·383– *j*0·006 |
| 0·275– *j*0·006 | –0·134– *j*0·016 | –0·141+ *j*0·024 |
| 0·248– *j*0·005 | 0·033+ *j*0·007 | 0·752+ *j*0·000 |

Current

| Mode 1 | Mode 2 | Mode 3 |
|---|---|---|
| 1·313+ *j*0·039 | 3·596– *j*0·494 | –0·585– *j*0·010 |
| 1·296+ *j*0·016 | –4·948+ *j*0·507 | –0·209+ *j*0·023 |
| 1·000+ *j*0·000 | 1·000+ *j*0·000 | 1·000+ *j*0·000 |

*Table 3·7: Derived parameters for electrically short lines at power frequency*

Series parameters, Ω/km

$$Z_1 = 0{\cdot}2165 + j\,0{\cdot}4643$$

$$Z_0 = 0{\cdot}3434 + j\,1{\cdot}2000$$

$$Z_{PP} = 0{\cdot}0423 + j\,0{\cdot}2452$$

$$Z_P = 0{\cdot}2588 + j\,0{\cdot}7095$$

Shunt parameters, F/km

$$C_1 = 7{\cdot}132 \times 10^{-9}$$

$$C_0 = 5{\cdot}618 \times 10^{-9}$$

$$C_{PP} = 79{\cdot}394 \times 10^{-9}$$

$$C_P = 6{\cdot}544 \times 10^{-9}$$

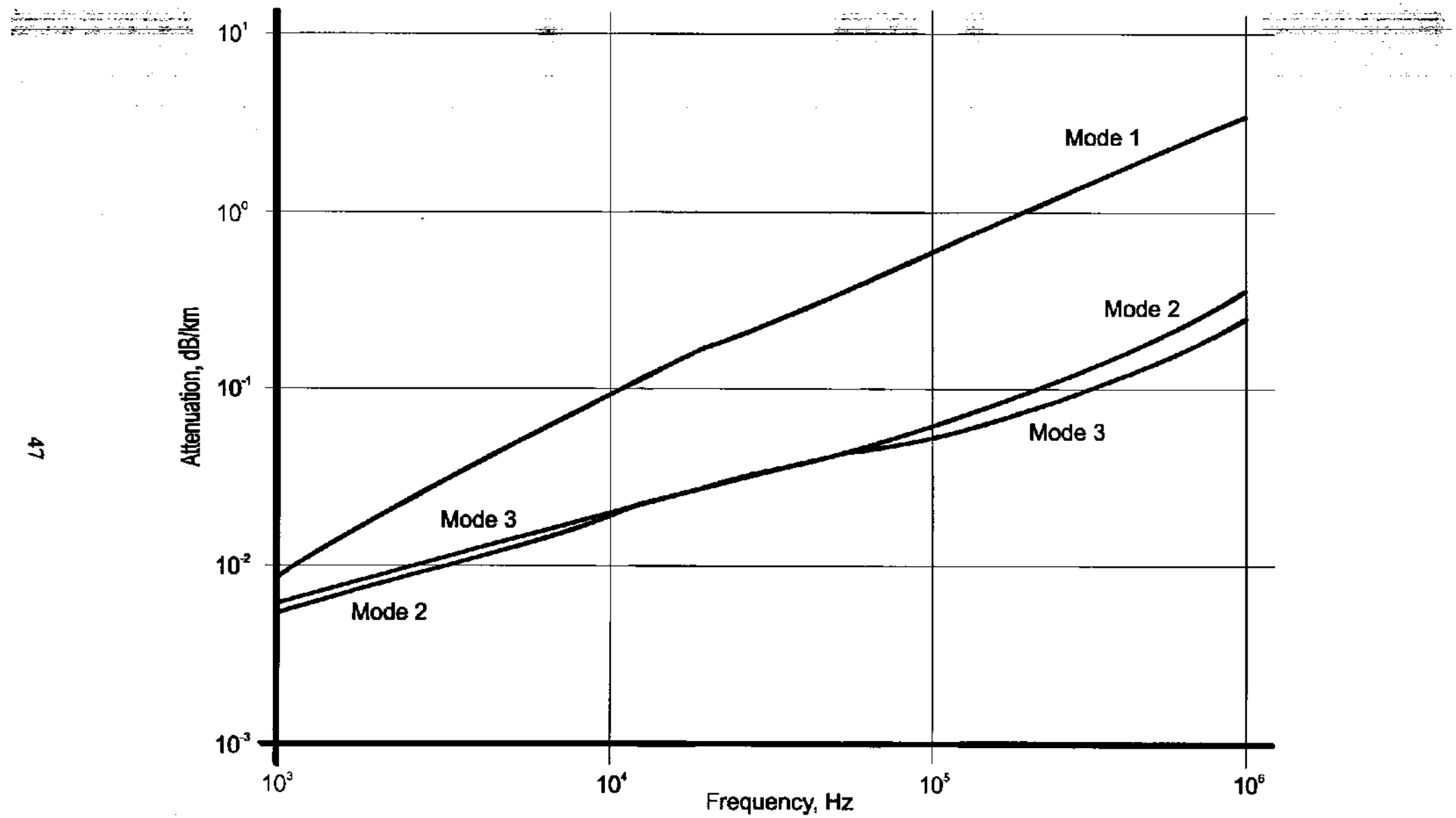



*Fig 3 4: Variation of attenuation with frequency*

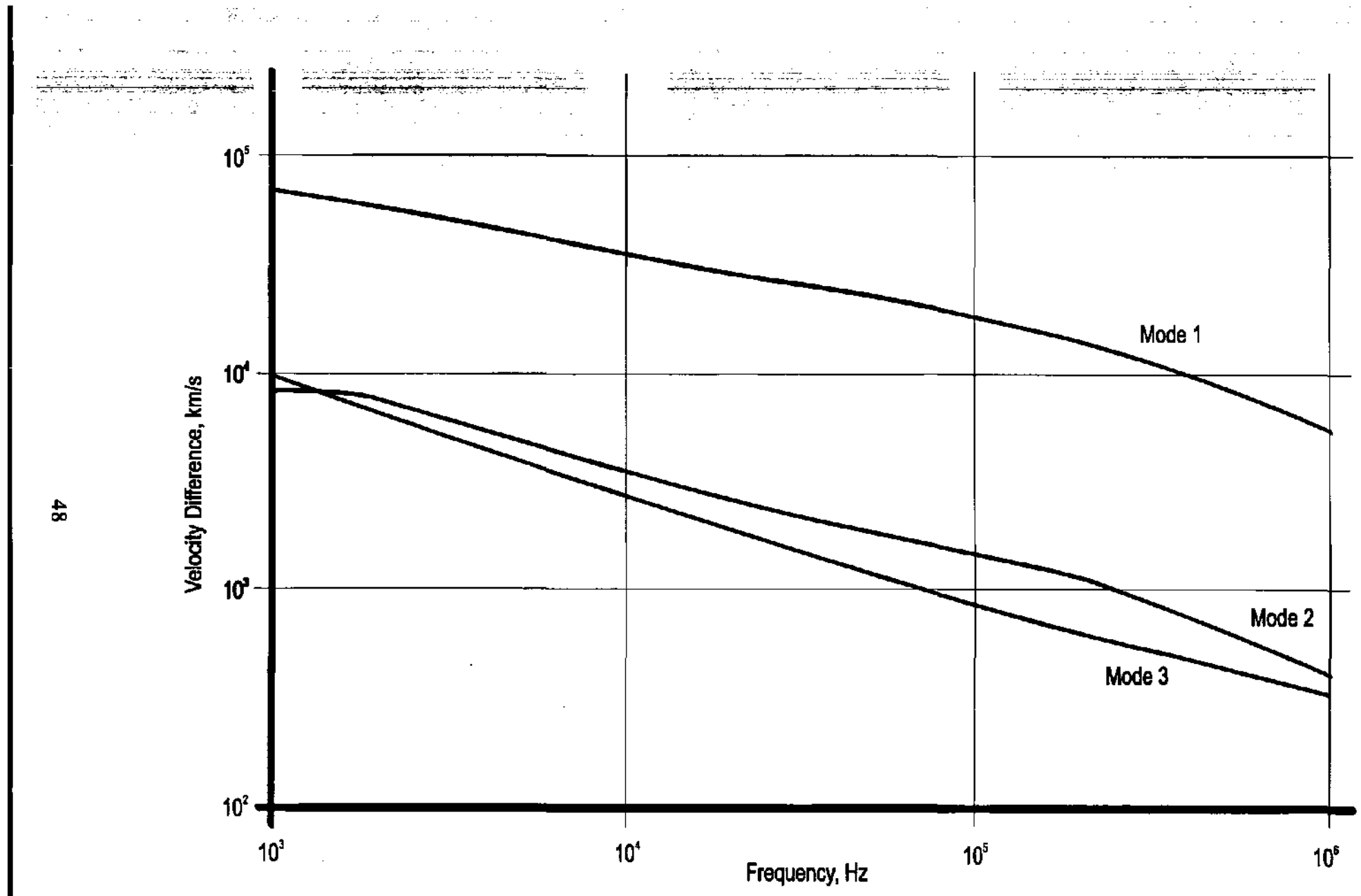



*Fig 3.5: Variation of velocity difference with frequency*

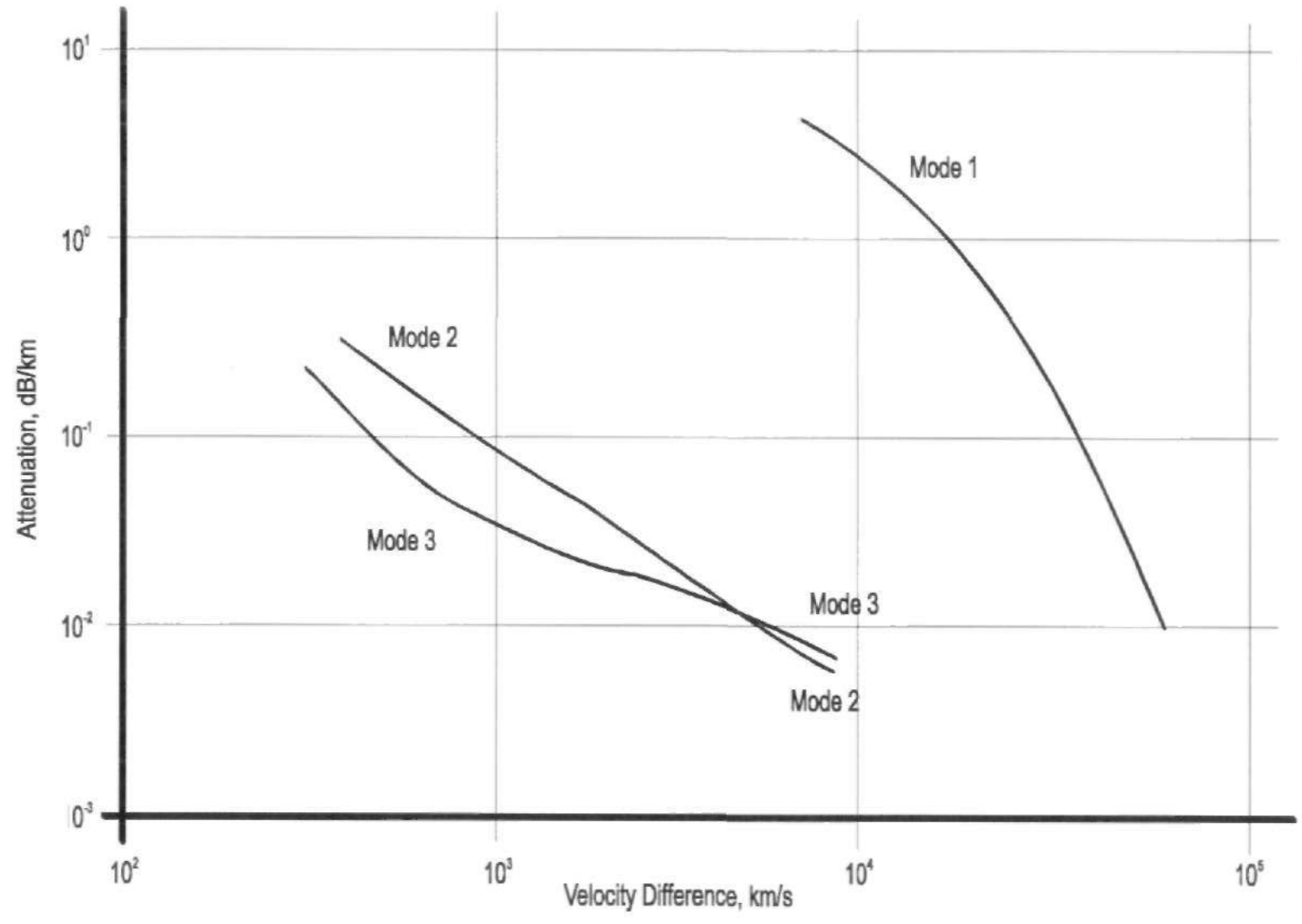



*Fig 3 6: Variation of attenuation with velocity difference*

# CHAPTER FOUR

## CONCLUSIONS AND RECOMMENDATIONS

### 4.1 CONCLUSIONS

The objectives of this research were defined as follows:

(1) Characterization of signal attenuation and propagation velocities on the Shiroro Complex 132kV lines;

(2) Identification of the frequencies at which significant power would be obtained at the receiving end.

From the results obtained, the following conclusions were drawn:

(1) Mode 3 has the least attenuation and a significant amount of power can be obtained between 1kHz and 500kHz;

(2) Mode 3 is less lossy than mode 2;

(3) Mode 1 has the highest attenuation which is abnormally high at about the frequency of 1MHz. This is also true for modes 2 and 3 at the same frequency. The high attenuation for mode 1 is due to the fact that it utilises the earth as a return path;

(4) Modes 2 and 3 are the aerial modes;

(5) The earth-return mode (Mode 1) has the least propagation velocity;

(6) The attenuations and propagation velocities of the aerial modes are approximately the same. Their attenuations are relatively small and they have high propagation velocities which on the average is about 98·48% of that of light in free space;

(7) The attenuation of the aerial modes are the same between the frequencies of 10kHz and 90·5kHz.

(8) Between the 36kHz and 500kHz which is the frequency range used by NEPA, the attenuation is between 0·028dB/km and 0.100dB/km while the propagation velocity is between 290360 km/s and 297500km/s;

(9) For the high frequency calculations, modes 2 and 3 are acceptable for frequencies in the kilo-

hertz range. Generally, by observing the range of frequencies considered in the high frequency calculations, one may conclude that as far as the Shiroro Complex 132kV lines are concerned, much power loss is associated with the mode 1 operation while mode 2 and mode 3 operations are acceptable when the frequency is in the kilohertz range;

(10) For the power frequency calculations, the earth-return path calculation gives a positive-sequence resistance, which is greater than the conductor resistance. In the analysis of carrier propagation problems, the positive-sequence resistance should be slightly greater than the conductor resistance if the earth-return path correction is used [10]. In this thesis, the positive-sequence resistance was found to be 0·2165Ω /km and the conductor resistance was found to be 0·1554Ω /km.

From the line data and the line configuration obtained from NEPA, this reaearch has established that the carrier performance is enhanced when the carrier frequencies is between 1kHz and 500kHz. The ESB500 powerline carriers which are manufactured by Siemens of Germany is now being used by NEPA for some of its Kaduna region installations especially the Shiroro Complex. The ESB powerline carrier frequency is between 36kHz and 500kHz which lies within the range established by this research. The objective of the research is therefore achieved.

## 4·2 RECOMMENDATIONS

(1) A computer program was developed to simplify the analytical rigours. This program could be modified to form an applications package which could be used extensively to study and analyse carrier propagation problems.

(2) The effects of the load currents of the four individual lines in the Shiroro Complex should be considered in a future research on this complex.

(3) Distortion to carrier channels may be caused by poor frequency response which is particularly detrimental to services employing frequency modulation. It therefore should be considered as necessary to measure the carrier frequency response of all newly installed carrier channels to ensure proper operation.

(4) Sufficient margin should be allowed in the design of powerline carriers so that weather and other environmental setbacks would not affect their operation adversely.

(5) Line traps should be inserted in series with tap lines for the given permissible attenuation for the bandwidth of any carrier channel on the through circuit so as to prevent high frequencies from passing through the transmission line.

(6) Assessment of carrier performance should be made on all installed carrier channels, especially, the newly installed ones, in order to be sure of proper powerline carrier operation.

(7) A great deal of thought should be devoted to the subject of carrier performance and adequate funds should be made available to support research and development in the subject. Communications System Reliability Studies should be conducted on the NEPA installations along the lines adopted in this project to ensure an in-depth appreciation of the NEPA Power System Communications as a whole.

(8) The management of NEPA, especially those in charge of transmission need to be fully aware and current about the subject of carrier propagation characteristics. They should strive for effective transfer of intelligence over 50 Hertz frequency as well as for the forms in which other powerlines are utilized in order to achieve a high reliability standard of communication. Therefore, the suggestions stated in item (7) should be included as part of the corporate policy and given top management attention.

(9) The characteristic impedance of a carrier circuit, very useful in powerline carrier studies may also be used to determine the restriking-voltage transients associated with circuit breakers clearing faults in powerlines. This restriking voltage which occurs during the critical period prior to the first reflection can be evaluated solely in terms of the characteristic-impedance matrix and the appropriate energization conditions. It is therefore recommended that such a study be undertaken as further research to this project.

(10) The current research has taken into cognisance, the most recently commissioned 132kV lines, that is, the Shiroro Complex. It is recommended that a similar research be carried out on its associated 330kV lines for greater coverage.

# REFERENCES


(1) R.G. Wasley: "*Intrabundle and power-line carrier loss characteristics including effects of height*". Proceedings IEE, Vol. 121, No. 6. pp. 432-434, June 1974.

(2) B.P. Belous, M.V. Kostenko and G.V. Mikutsky: "*Investigation and calculation of high frequency paths of communication channels of transmission lines*". CIGRE Proceedings, Art. 382. 1966.

(3) W.H. Senn and K.P. Morf: "*Optimum power-line carrier coupling arrangement on transposed single circuit power lines*". CIGRE Proceedings, Art 35. February, 1974.

(4) L.S. Perelman: "*An effect of conductor sagging upon wave propagation along a transmission line*". Elektrichestvo, No. 2. 1968.

(5) M.Kh. Zakar-Itkin: "*On the matrix telegraph equations of wave propagation along inhomogeneous multi-conductor lines*". Elektrichestvo, No. 2, pp. 60-69. 1969.

(6) M.C. Perz and R.L. Hazel: "*Effects of earth resistivity on modal parameters of an extra high voltage horizontal line at power-line carrier frequencies*". IEEE Transactions on Power Apparatus and Systems, Vol. PAS 88.

(7) S. Christina and M. D'Amore: "*Performance sensitivity of a power-line carrier channel*". IEEE Transactions on Power Apparatus and Systems, Vol. PAS 98, No. 4, pp. 1337-1344. 1979.

(8) S. Christina and M. D'Amore: "*A new efficient method to evaluate carrier channel performances on long extra high voltage power lines with transpositions*". IEEE Transactions on Power Apparatus and Systems, Vol. PAS 101, No. 9, pp. 3053-3060. September, 1982.

(9) L.M. Wedepohl: "*Application of Matrix Methods to the solution of travelling - wave phenomena in polyphase systems*". Proceedimgs IEE, Vol. 110, pp. 2200-2212. December, 1963.

(10) R.H. Galloway, W.B. Shorrocks and L.M. Wedepohl: "*Calculation of electrical parameters for short and long polyphase transmission lines*". Proceedings IEE, Vol. 111, No. 12, pp. 2051-2059. December, 1964.

(11) C.S. Indulkar, Parmod Kumar and D.P. Kothari: "*Some Studies on Carrier Propagation in Overhead Transmission Lines*". IEEE Transactions on Power Apparatus and Systems, Vol. PAS 102, No. 4. April, 1983.

(12) J.R. Carson: "*Wave propagation in overhead wires with ground return*". Bell Systems Technical J. Vol. 5, pp. 539. 1926.

(13) S. Butterworth: "Electrical Characteristics of overhead lines". ERA, 1954, pp 13.

# APPENDICES


Appendix A: Line impedances for Kaduna Region 132 kV circuits - 56

Appendix B: Line parameters for Shiroro Complex 132 kV lines - 57

Appendix C: Configuration of Shiroro Complex 132 kV line - 58

Appendix D: Program PLC_SHIR - 59

Appendix E: Map of Nigeria showing the NEPA grid system - 71

Appendix F: System flow sheet for Kaduna Region - 72

| Line Name | Type | Line Length (km) | Positive Sequence Impedance (Ohms) | Zero Sequence Impedance (Ohms) |
|---|---|---|---|---|
| Kaduna-Kaduna Town | DC-WOLF | 12 | 5.95/69° | 18.40/74° |
| Kaduna-Zaria | DC-WOLF | 72 | 33.95/69° | 115.90/74° |
| Zaria-Sokoto | DC-WOLF | 303 | 167.00/69° | 584.51/74° |
| Zaria-Kano | DC-WOLF | 145 | 66.02/69° | 232.46/74° |
| Kano-Dankata | DC-WOLF | 12 | 5.50/69° | 17.07/71° |
| Kano-Katsina | DC-WOLF | 130 | 60.15/69° | 255.98/74° |
| Kano-Dan Agundi | DC-WOLF | 8 | 3.70/69° | 12.98/74° |
| Dankata-Hadejia | DC-WOLF | 150 | 64.95/69° | 211.93/74° |
| Jos-Bauchi | DC-WOLF | 118 | 54.50/69° | 190.00/74° |
| Bauchi-Gombe | DC-WOLF | 146 | 67.45/69° | 235.10/74° |
| Gombe-Yola | DC-WOLF | 216 | 99.70/69° | 347.30/74° |
| Gombe-Biu | DC-WOLF | 126 | 58.21/69° | 202.89/74° |
| Gombe-Potiskum | DC-WOLF | 101 | 93.61/69° | 221.46/74° |
| Biu-Maiduguri | DC-WOLF | 177 | 80.30/69° | 255.00/74° |
| Shiroro-Minna | DC-WOLF | 58 | 26.25/69° | 90.37/74° |
| Shiroro-Tegina | DC-WOLF | 75 | 30.83/69° | 104.66/74° |
| Tegina-Kontagora | DC-WOLF | 100 | 46.00/69° | 161.02/74° |
| Kontagora-Yelwa | DC-WOLF | 102 | 50.35/69° | 175.51/74° |
| Minna-Bida | DC-WOLF | 90 | 41.58/69° | 144.32/74° |
| Minna-Abuja | DC-WOLF | 136 | 62.22/69° | 193.41/74° |

APPENDIX A2 (Cont'd) to Zaria-Kano Report (ECN Transmission)

56

National Electric Power Authority
Transmission Division
Kaduna Road
P.M.B. 01
Kaduna

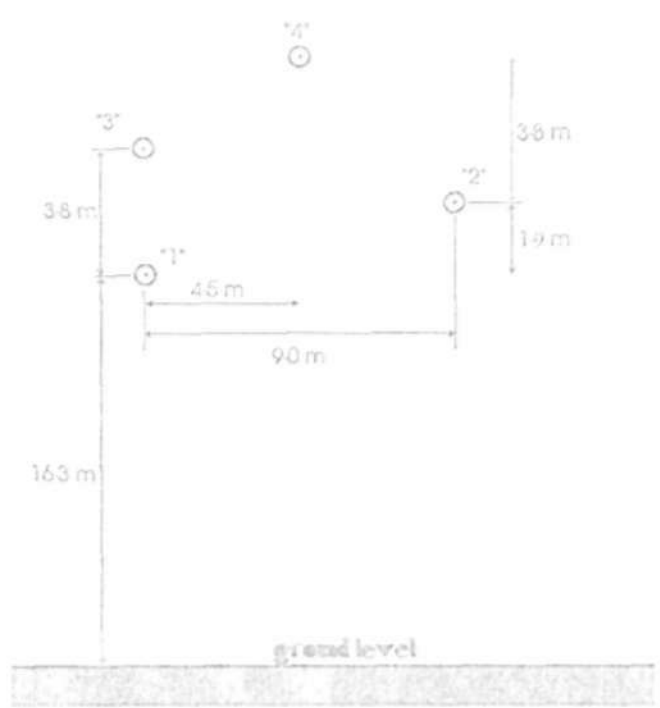
| S/No | PARAMETER | SPECIFICATION |
|---|---|---|
| 1 | Positive-sequence impedance, $Z_1$ | 0.1037 + j 0.41390/km |
| 2 | Negative-sequence impedance, $Z_2$ | 0.1037 + j 0.41390/km |
| 3 | Zero-sequence impedance, $Z_0$ | 0.2353 + j 1.30490/km |
| 4 | Mutual capacitance, $C_m$ | $1.12 \times 10^{-8}$ F/km |
| 5 | Operating capacitance, $C_1$ | $8.82 \times 10^{-9}$ F/km |
| 6 | Capacitance-to-earth, $C_0$ | $5.45 \times 10^{-9}$ F/km |
| 7 | Surge impedance, Z | 306.47 Ω |
| 8 | Surge capacity, $P_0$ | 45.00 MW |
| 9 | Charging capacity, $P_c$ | 0.0133 MVAR/km |
| 10 | Charging current, $I_c$ | 0.251 A/km |
| 11 | Earth-leakage current, $I_e$ | 0.331 A/km |
| 12 | Maximum boundary field strength, E | 22.2kV |
| 13 | Conductor type | ACSR (WOLF) |
| 14 | Conductor size, CSA | 134.4 mm² |
| 15 | Load current, $I_{nc}$ | 170 A |
| 16 | Load current, $I_{sc}$ | Not available |
| 17 | Load current, $I_{cc}$ | 40 A |
| 18 | Load current, $I_{op}$ | 720 (MVA) |
| 19 | Weight of conductor | Steel core covered |
| 20 | Protecting treatment | Steel |
| 21 | Earth wire type | 35.5 mm² |
| 22 | Earth wire size, CSA | Single ea 4b wire 30° |
| 23 | Shielding/shielding angle | 300 |
| 24 | Maximum SC time | 220 - 400 kV (0.4 - 0.2 s) |
| 25 | Design life | 50 yr |
| 26 | Maximum height above | 24.2 m (300kV) - 42.1 m(330kV) |
| 27 | Weight of tower | 67 kg/m |
| 28 | Body extension | 132 kV |
| 29 | Voltage level | |

*APPENDIX B: Line parameters for 30, Shiroro Complex 132kV lines*

National Electric Power
Transmission Dept.
Mando Road,
P. M. B. 2182
Kaduna.

*APPENDIX B (cont): Line parameters for Shiroro Complex 132 kV lines*

| Parameter | Specification |
|---|---|
| Aluminium CSA | 150·0 mm² |
| Aluminium Strands | 30 |
| Steel CSA | 44·9 mm² |
| Steel Strands | 7 |




*APPENDIX C: Configuration of Shiroro Complex 132 kV line*

National Electric Power
Transmission Department
Mando Road
P.M.B. 2136
Kaduna

```
C     PROGRAM IDENTIFICATION
C     PROGRAM NAME: PLC_SHIR
C     THIS PROGRAM COMPUTES THE POWERLINE CARRIER PROPAGATION
C     CHARACTERISTICS OF THE SHIRORO COMPLEX 132kV LINES
C     **********  CONSTANTS IDENTIFICATION  ************
C     RHO1   : EARTH RESISTIVITY
C     RHO2   : CONDUCTOR RESISTIVITY
C     RHO3   : EARTHWIRE RESISTIVITY
C     MU     : EARTH PERMEABILITY
C     EXPS   : PERMITTIVITY OF FREE SPACE
C     CONV   : DEGREES TO RADIANS CONVERSION CONSTANT
C     K      : CONDUCTOR STRANDING FACTOR
C     PI     : CONSTANT 3.14159
C     GAMMA  : EULER'S CONSTANT
C     C      : FREE SPACE VELOCITY
C     **********  CONSTANTS INITIALISATION  *************
      RHO1=100.0
      RHO2=3.82E-8
      RHO3=20.E-8
      MU=4.*PI*1.E-7
      EXPS=8.854E-12
      CONV=PI/180.
      K=2.25
      PI=3.14159
      GAMMA=1.7811
      C=3.0E-8
C     ***********  VARIABLES IDENTIFICATION  *************
C     Y      : SHUNT ADMITTANCE MATRIX
C     Z      : SERIES ADMITTANCE MATRIX
C     ZINMO  : INVERSE OF Z
C     XG     : REACTANCE DUE TO PHYSICAL GEOMETRY
C     RC,XC  : RESISTANCE,REACTANCE DUE TO CONDUCTOR
C     RC,XC  : RESISTANCE,REACTANCE DUE TO EARTH-RETURN PATH
C     DBC    : DISTANCE BETWEEN CONDUCTOR i AND CONDUCTOR j
C     DBCI   : DISTANCE BETWEEN CONDUCTOR j AND IMAGE OF CONDUCTOR i
C     BETA   : ANGLE SUBTENDED BETWEEN LINE DBC AND LINE DBCI
C     BETAA  : PHASE CONSTANT OR VELOCITY FACTOR
C     THETA  : ANGLE SUBTENDED BETWEEN DBCI AND CONDUCTOR j
C     ALPHA  : ANGLE SUBTENDED BETWEEN DBC AND CONDUCTOR i
C     ALPHAA: ATTENUATION CONSTANT
C     MUU    : MODE VELOCITY
C     B      : CHARGE-COEFFICIENT MATRIX
C     BIN    : INVERSE OF B
C     BINMO  : MODIFIED INVERSE OF B
C     YIN    : INVERSE OF Y
C     Z1     : POSITIVE SEQUENCE IMPEDANCE
C     Z0     : ZERO SEQUENCE IMPEDANCE
C     ZP     : EARTH-LOOP IMPEDANCE
C     ZPP    : INTERPHASE MUTUAL IMPEDANCE
C     C1     : POSITIVE SEQUENCE CAPACITANCE
C     C0     : ZERO SEQUENCE CAPACITANCE
C     CP     : EARTH-LOOP CAPACITANCE
C     CPP    : INTERPHASE MUTUAL CAPACITANCE
C     PC     : COMPLEX MATRIX FORMED BY [Y]*[Z]
```

```
C     OMEGA : ANGULAR FREQUENCY
C     F     : FREQUENCY
C     P     : REAL CORRECTION COMPONENT
C     Q     : IMMAGINARY CORRECTION COMPONENT
C     QC    : MODE DISTRIBUTION OF VOLTAGE
C     S     : MODE DISTRIBUTION OF CURRENT
C     Z0    : CHARACTERISTIC IMPEDANCE MATRIX
C     Y0    : CHARACTERISTIC ADMITTANCE MATRIX
C     dV    : VELOCITY DIFFERENCE
C     S2,S2P,S4,S4P,SG1,SG2,SG3 and SG4 are infinite series(constants)
C     AN,CN,EN,FN,GN and HN are terms of a sequence
C     **********  SUBROUTINES IDENTIFICATION  ***********
C     ADMAT : CALCULATES ADMITTANCE MATRIX
C     BIMMAT: CALCULATES IMPEDANCE MATRIX
C     LUBKSB: PERFORMS BACK SUBSTITUTION INTO A MATRIX
C     LUDCMP: DECOMPOSE MATRIX
C     JACOBI: FINDS EIGENVALUES AND EIGENVECTORS
C     CONAN : CALCULATES TERM AN
C     CONCN : CALCULATES TERM CN
C     CONEN : CALCULATES TERM EN
C     CONFN : CALCULATES TERM FN
C     CONGN : CALCULATES TERM GN
C     CONHN : CALCULATES TERM HN
C     CONS2 : FINDS ELEMENTS AND SUM OF SERIES S2
C     CONS2P: FINDS ELEMENTS AND SUM OF SERIES S2P
C     CONS4 : FINDS ELEMENTS AND SUM OF SERIES S4
C     CONS4P: FINDS ELEMENTS AND SUM OF SERIES S4P
C     CONSG1: FINDS ELEMENTS AND SUM OF SERIES SG1
C     CONSG2: FINDS ELEMENTS AND SUM OF SERIES SG2
C     CONSG3: FINDS ELEMENTS AND SUM OF SERIES SG3
C     CONSG4: FINDS ELEMENTS AND SUM OF SERIES SG4
C     INVERSE: COMPUTES THE INVERSE OF A MATRIX
C     IMPC    : CALCULATES THE RESIETANCE AND THE REACTANCE DUE TO CONDUCTOR
C     IMPE    : CALCULATES THE RESISTANCE AND THE REACTANCE DUE TO THE EARTH
C          RETURN PATH
C     REAG    : CALCULATES THE REACTANCE DUE TO THE PHYSICAL GEOMETRY OF THE
C          CONDUCTORS
C     ************  TYPE DECLARATION  ************
      COMPLEX Y,XE,XG,XC,YIN,PC
C     **************  MAIN PROGRAM  **************
      M=3
      N=4
      NP=4
      CALL ADMAT(Y,N,NP,B)
      READ(*,*)F,THETA
      DO 6 I=1,N
      CALL BIMMAT(Z,N,M,XG,RC,RE,XE,XC)
      CALL DEPARM(ZINMO,YIN,M,Z1,Z0,ZP,ZPP,C1,C0,CP,CPP)
    6 CONTINUE
      STOP
      END
```

```
      SUBROUTINE DEPARM (ZINMO,YIN,M,Z1,Z0,ZP,ZPP,C1,C0,CP,CPP)
C     THIS ROUTINE CALCULATES AND PRINTS ALL DESIRED DERIVED PARAMETERS
      Z1 = (ZINMO(1,1)+ZINMO(2,2)+ZINMO(3,3)-ZINMO(1,2)-ZINMO(1,3)
     4-ZINMO(2,3))/3.
      Z0 = (ZINMO(1,1)+ZINMO(2,2)+ZINMO(3,3)+ZINMO(1,2)+ZINMO(1,3)
     5+ZINMO(2,3))/3.
      ZPP = (Z0-Z1)/3.
      ZP  = Z1+ZPP
      C1 = 3./(OMEGA*(YIN(1,1)+YIN(2,2)+YIN(3,3)-YIN(1,2)-YIN(2,3)
     6-YIN(1,3)))
      C0 = 3./(OMEGA*(YIN(1,1)+YIN(2,2)+YIN(3,3)+2.*YIN(1,2)+2.*
     7YIN(1,3)+2.*YIN(2,3)))
      CPP = 1./((1./C0)-(1./C1))
      CP  = 1./((1./C1)+(1./CPP))
      CALL MATMUL(PC,ADMAT,Z,M)
      CALL JACOBI(A,N,NP,D,V,NROT)
      CALL INVERSE(GAMMA,GAMM,INDX)
      CALL MATMUL(RE1,Q,GAMM,M)
      CALL INVERSE(Q,Q1,INDX)
      CALL MATMUL(RE2,RE1,Q1,M)
      CALL MATMUL(Z0,RE2,Z,M)
      CALL MATMUL(Y0,RE2,Y,M)
C     TRANSPOSE MATRIX
      DO 74 I = 1,N
      DO 74 J = 1,N
      V(J,IP) = V(IP,J)
      V(J,IQ) = V(IQ,J)
 74   CONTINUE
      DO 77 I = 1,N
      DO 77 J = 1,N
      A(I,J) = V(IP,J)
 77   CONTINUE
      CALL INVERSE(A,Y,INDX)
      DO 78 I = 1,N
      DO 78 J = 1,N
      S(I,J) =Y(I,J)
 78   CONTINUE
      DO 81 I = 1,N
      DO 81 J = 1,N
      A(I,J) = V(IQ,J)
 81   CONTINUE
      CALL INVERSE(A,Y,INDX)
      DO 84 I = 1,N
      DO 84 J = 1,N
      S(I,J) = Y(I,J)
 84   CONTINUE
      WRITE(*,96)
 96   FORMAT(15X,"SERIES PARAMETERS")
      WRITE(*,91)Z1
 91   FORMAT(10X,"POSITIVE SEQUENCE IMPEDANCE, Z1=",F6.4,3X,"OHM/METER"/
     6)
      WRITE(*,92)Z0
 92   FORMAT(10X,"ZERO SEQUENCE IMPEDANCE, Z0=",F6.4,3X,"OHM/METER"/)
      WRITE(*,93)ZPP
 93   FORMAT(10X,"INTERPHASE MUTUAL IMPEDANCE, ZPP=",F6.4,3X,"OHM/METER"
     7/)
      WRITE(*,94)ZP
 94   FORMAT(10X,"EARTH-LOOP IMPEDANCE, ZP=",F6.4,3X,"OHM/METER"/)
      WRITE(*,95)
 95   FORMAT(15X,"SHUNT PARAMETERS")
```

```
      WRITE(*,97)C1
   97 FORMAT(10X,"POSITIVE SEQUENCE CAPACITANCE, C1=",F7.4,3X,"FARAD/MET
     8ER"/)
      WRITE(*,98)C0
   98 FORMAT(10X,"ZERO SEQUENCE CAPACITANCE, CO=",F7.4,3X,"FARAD/METER"/
     9)
      WRITE(*,99)CPP
   99 FORMAT(10X,"INTERPHASE MUTUAL CAPACITANCE, CPP=",F7.4,3X,"FARAD/ME
     ATER"/)
      WRITE(*,100)CP
  100 FORMAT(10X,"EARTH-LOOP CAPACITANCE, CP=",F7.4,3X,"FARAD/METER"/)
      RETURN
      END


      SUBROUTINE ADMAT(X1,X2,Y1,Y2,THETA,A,C,Y,INDX,YM)
      DIMENSION A(NP,NP),C(NP,NP),Y(NP,NP),INDX(N),YM(M,M)
      DO 10 I=1,N
      DO 10 J=1,N
      READ(*,90) X1,X2,Y1,Y2,THETA,F
   90 FORMAT(1X,'ENTER X AXIS COORDINATES='2A2,' Y AXIS COORDINATES
     S ='',2A2,'AND SIZE OF ANGLES='',F4)
      DBC(I,J)=SQRT((X1-X2)**2+(Y1-Y2)**2)
      BETA=ASIN((SIN(THETA*CONV)*2.*Y1)/DBCI(I,J)
      ALPHA=180.-(THETA+BETA)
      DBCI(I,J)=SQRT(DBC**2+2.*Y1**2-2.*DBC*2.*Y1*COS(ALPHA*CONV))
      C(I,J)=LOG(DBCI/DBC)
      A(I,J)=C(I,J)
   10 CONTINUE
C     FIND INVERSE
      DO 12 I=1,N
      DO 11 J=1,N
      Y(I,J)=0.
   11 CONTINUE
      Y(I,I)=1.
   12 CONTINUE
      CALL LUDCMP(A,N,NP,INDX,D)
      DO 21 J=1,N
      CALL LUBKSB(A,N,NP,INDX,Y(I,J))
   21 CONTINUE
      Y(1,4)=0.
      Y(2,4)=0.
      Y(3,4)=0.
      Y(4,4)=0.
      Y(4,1)=0.
      Y(4,2)=0.
      Y(4,3)=0.
      DO 22 I=1,M
      DO 22 J=1,M
      YM(I,J)=Y(I,J)
      ADMAT=j*PI*EXPS*OMEGA*2.*YM
      A(I,J)=ADMAT
   22 CONTINUE
      CALL INVERSE(A,Y,INDX)
      DO 88 I = 1,N
      DO 88 J = 1,N
      YIN(I,J) =Y(I,J)
   88 CONTINUE
      RETURN
      END
```

```
      SUBROUTINE BIMMAT(Z,ZINMO,N,M,XG,RC,RE,XE,XC)
      DIMENSION Z(N,N),ZINMO(M,M),XG(N,N),RC(N,N),XC(N,N),RE(N,N),
     X     XE(N,N)
      OMEGA = 2.*PI*F
      CALL REAG(C,XG)
      CALL IMPC(NO,RO,RC,XC)
      CALL IMPE(DBCI,F,THETA)
      DO 28 I = 1,N
      DO 28 J = 1,N
      ZRES(I,J) = RE(I,J)+RC(I,J)
      ZREAC(I,J) = XG(I,J)+XC(I,J)+XE(I,J)
      Z(I,J) = ZRES(I,J)+j*ZREAC(I,J)
      A(I,J) = Z(I,J)
   28 CONTINUE
      CALL INVERSE(A,Y,INDX)
      Y(1,4) = 0.
      Y(2,4) = 0.
      Y(3,4) = 0.
      Y(4,4) = 0.
      Y(4,3) = 0.
      Y(4,2) = 0.
      Y(4,1) = 0.
      DO 31 I = 1,M
      DO 30 J = 1,M
      A(I,J) = Y(I,J)
   30 CONTINUE
   31 CONTINUE
      CALL INVERSE(A,Y,INDX)
      DO 34 I = 1,M
      DO 33 J = 1,M
      ZINMO =Y(I,J)
   33 CONTINUE
   34 CONTINUE
      RETURN
      END


      SUBROUTINE CONAN(AN)
      DIMENSION AN(16)
      AN(0)=R**2/8.
      DO 42 N=1,16
      AN(N)=-(AN(N-1)/(2.*N*(2.*N+1.)**2*(2.*N+2.))*R**4/2.
   42 CONTINUE
      RETURN
      END


      SUBROUTINE CONCN(CN)
      DIMENSION CN(16)
      CN(0)=R**4/192.
      DO 43 N=1,16
      CN(N)=-(CN(N-1)/(2.*N+1.)*(2.*N+2.)**2*(2.*N+3.))*R**4/2.
   43 CONTINUE
      RETURN
      END
```

```
      SUBROUTINE CONEN(EN)
      DIMENSION EN(16)
      EN(0)=R/3.
      DO 44 N=1,16
      EN(N)=-(EN(N-1)/4.*N-1.)*(4.*N+1.)**2*(4.*N+3))*R**4
   44 CONTINUE
      RETURN
      END

      SUBROUTINE CONFN(FN)
      DIMENSION FN(16)
      FN(0)=R**3/45.
      DO 45 N=1,16
      FN(N)=-(FN(N-1)/(4.*N+1)*(4.*N+3.)**2*(4.*N+5.))*R**4
   45 CONTINUE
      RETURN
      END


      SUBROUTINE CONGN(GN)
      DIMENSION GN(16)
      GN(0)=5./4.
      DO 46 N=1,16
      GN(N)=GN(N-1)+(1./(4.*N+2.)+1./(4.*N+2.)+1./(2.*N+1)+1./(2.*N+2.)
     3 +1./(4.*N+4.))
   46 CONTINUE
      RETURN
      END


      SUBROUTINE CONS4(CN,S4,THETA)
      DIMENSION CN(16),S4(16)
      S4(N)=0.
      CALL CONAN(AN)
      DO 50 N=1,16
      S4(N)=S4(N)+(CN(N)*COS(4.*N+4.)*THETA*CONV)
   50 CONTINUE
      RETURN
      END

      SUBROUTINE CONS4P(CN,S4P,THETA)
      DIMENSION NC(16),S4P(16)
      S4P(N)=0.
      CALL CONCN(CN)
      DO 51 N=1,16
      S4P(N)=S4P(N)+CN(N)*SIN(4.*N+4.)*THETA*CONV)
   51 CONTINUE
      RETURN
      END


      SUBROUTINE CONSG1(EN,SG1,THETA)
      DIMENSION EN(16),SG1(16)
      SG1(N)=0.
      CALL CONEN(EN)
      DO 52 N=1,16
      SG1(N)=SG1(N)+(EN(N)*COS(4.*N+1.)*THETA*CONV)
   52 CONTINUE
      RETURN
      END
```

```
      SUBROUTINE CONSG2(GN,SG2,THETA)
      DIMENSION GN(16),SG2(16)
      SG2(N)=0.
      CALL CONGN(GN)
      CALL CONS2(AN,S2,THETA)
      DO 53 N=1,16
      SG2(N)=SG2(N)+(GN(N)*S2(N))
   53 CONTINUE
      END

      SUBROUTINE CONHN(HN)
      DIMENSION HN(16)
      HN(0)=5./3.
      DO 47 N=1,16
      HN(N)=HN(N-1)+1./(4.*N+2.)+1./(2.*N+2.)+1./(2.*N+3.)-1./(4.*N+6.)
   47 CONTINUE
      RETURN
      END

      SUBROUTINE CONS2(AN,S2,THETA)
      DIMENSION AN(16),S2(16)
      S2(N)=0.
      CALL CONAN(AN)
      DO 48 N=1,16
      S2(N)=S2(N)+(AN(N)+COS(4.*N+2)*THETA*CONV)
   48 CONTINUE
      RETURN
      END
```

```
      SUBROUTINE CONSG3(FN,SG3,THETA)
      DIMENSION SG3(16),FN(16)
      SG3(N)=0.
      CALL CONFN(FN)
      DO 54 N=1,16
      SG3(N)=SG3(N)+FN(N)*COS((4.*N+3.)*CONV)*THETA
   54 CONTINUE
      RETURN
      END

      SUBROUTINE CONSG4(HN,SG4,THETA)
      DIMENSION HN(16), SG4(16)
      SG4(N)=0.
      CALL CONHN(HN)
      CALL CONS4(CN,S4,THETA)
      DO 55 N=1,16
      SG4(N)=SG4(N)+HN(N)*S4(N)
   55 CONTINUE
      RETURN
      END

      SUBROUTINE CONS2P(AN,S2P,THETA)
      DIMENSION AN(16),S2P(16)
      S2P(N)=0.
      CALL CONAN(AN)
      DO 49 N=1,16
      S2P(N)=S2P(N)+(AN(N)*SIN(4.*N+2.)*THETA*CONV)
   49 CONTINUE
      RETURN
      END
```

```
      SUBROUTINE IMPC(NO,R,RC,XC)
      DIMENSION RC(N,N),XC(N,N)
      COMPLEX j,MS
      j=SQRT(-1)
      NO=30
      R=1.262E-3

C     NO is the number of strands in the conductor outer layer while
C     R is the radius of each outer strand

      MS=SQRT(j*OMEGA*MU/RHO2)
      DO 41 I=1,N
      DO 41 J=1,N
      RC=K*RHO2*MS/(SQRT(2.)*R*(NO+2)*PI)
      XC=RC
 41   CONTINUE
      RETURN
      END
```

```
      SUBROUTINE IMPE(R,DBCI,F,THETA,RE,XE)
      DIMENSION R(N,N),DBCI(N,N),RE(N,N),XE(N,N)
      DO 57 I=1,N
      DO 57 J=1,N
      R(I,J)=SQRT(OMEGA*MU/RHO1)/DBCI(I,J)
 57   CONTINUE
      CALL CONS2(AN,S2,THETA)
      CALL CONS2P(AN,S2P,THETA)
      CALL CONS4(CN,S4,THETA)
      CALL CONS4P(CN,S4P,THETA)
      CALL CONSG1(EN,SG1,THETA)
      CALL CONSG2(GN,SG2,THETA)
      CALL CONSG3(FN,SG3,THETA)
      CALL CONSG4(HN,SG4,THETA)
      DO 58 I=1,N
      DO 58 J=1,N
      IF(R(I,J).LE.5.) THEN
      P(I,J)=PI*(1-S4(I,J))/8.+0.5*S2(I,J)*LOG(2./(GAM*R(I,J))+0.5*THETA
     A*S2P(I,J)-SG1(I,J)/SQRT(2)+0.5*SG2(I,J)+SG3(I,J)/SQRT(2)
      Q(I,J)=0.25+0.5*LOG(2./(GAM*R(I,J))*(1-S4(I,J))-0.5*THETA*S4P(I,J)
     B+SG1(I,J)/SQRT(2)-PI*S2(I,J)/8.+SG3(I,J)/SQRT(2)-0.5*SG4(I,J)
      ELSE
      P(I,J)=COS(THETA*CONV)/(SQRT(2)*R(I,J))-COS(2.*THETA*CONV)/R(I,J)*
     C*2+COS(3.*THETA*CONV)/(SQRT(2)*R(I,J)**3)+3.*COS(5.*THETA*CONV)/(S
     DQRT(2)*R(I,J)**5)
      Q(I,J)=COS(THETA*CONV)/(SQRT(2)*R(I,J))-COS(3.*THETA*CONV)/(SQRT(2
     E)*R(I,J)**3)+3.*COS(5.*THETA*CONV)/(SQRT(2)*R(I,J)**5)
      END IF
      RE(I,J)=2.*P(I,J)*OMEGA*MU/(2.*PI)
      XE(I,J)=2.*Q(I,J)*OMEGA*MU/(2.*PI)
 58   CONTINUE
      RETURN
      END
```

```
      SUBROUTINE INVERSE(A,Y,INDX)
      DIMENSION A(NP,NP),Y(NP,NP),INDX(NP)
      DO 36 I=1,N
      DO 35 J=1,N
      Y(I,J)=0.
   35 CONTINUE
      Y(I,J)=1.
   36 CONTINUE
      CALL LUDCMP(A,N,NP,INDX,D)
      DO 37 J=1,N
      CALL LUBKSB(A,N,NP,INDX,Y(I,J))
   37 CONTINUE
      RETURN
      END


      SUBROUTINE LUDCMP(A,N,NP,INDX,D)
      PARAMETER(NMAX=100,TINY=1.0E-20)
      D0 12 I=1,N
      AAMAX=0.
      DO 11 J=1,N
      IF(ABS(A(I,J)).GT.AAMAX) AAMAX=ABS(A(I,J))
   11 CONTINUE
      IF(AAMAX.EQ.0.) PAUSE 'Singular Matrix'
      VV(I)=1./AAMAX
   12 CONTINUE
      DO 19 J=1,N
      DO 14 I=1,J-1
      SUM=A(I,J)
      DO 13 K=1,I-1
      SUM=SUM-A(I,K)*A(K,J)
   13 CONTINUE
      A(I,J)=SUM
   14 CONTINUE
      AAMAX=0.
      DO 16 I=J,N
      SUM=A(I,J)
      DO 15 K=1,J-1
      SUM=SUM-A(I,K)*A(K,J)
   15 CONTINUE
      A(I,J)=SUM
      DUM=VV(I)**ABS(SUM)
      IF(DUM.GE.AAMAX) THEN
      IMAX=I
      AAMAX=DUM
      END IF
   16 CONTINUE
      IF(J.NE.IMAX) THEN
      DO 17 K=1,N
      DUM=A(IMAX,K)
      A(IMAX,K)=A(J,K)
      A(J,K)=DUM
   17 CONTINUE
      D=-D
      VV(IMAX)=VV(J)
      END IF
      INDX(J)=IMAX
      IF(A(J,J).EQ.0.) A(J,J)=TINY
      IF(J.NE.N) THEN
```

```
      DUM=1./A(J,J)
      D0 18 I=J+1,N
      A(I,J)=A(I,J)*DUM
   18 CONTINUE
      END IF
   19 CONTINUE
      RETURN
      END
```

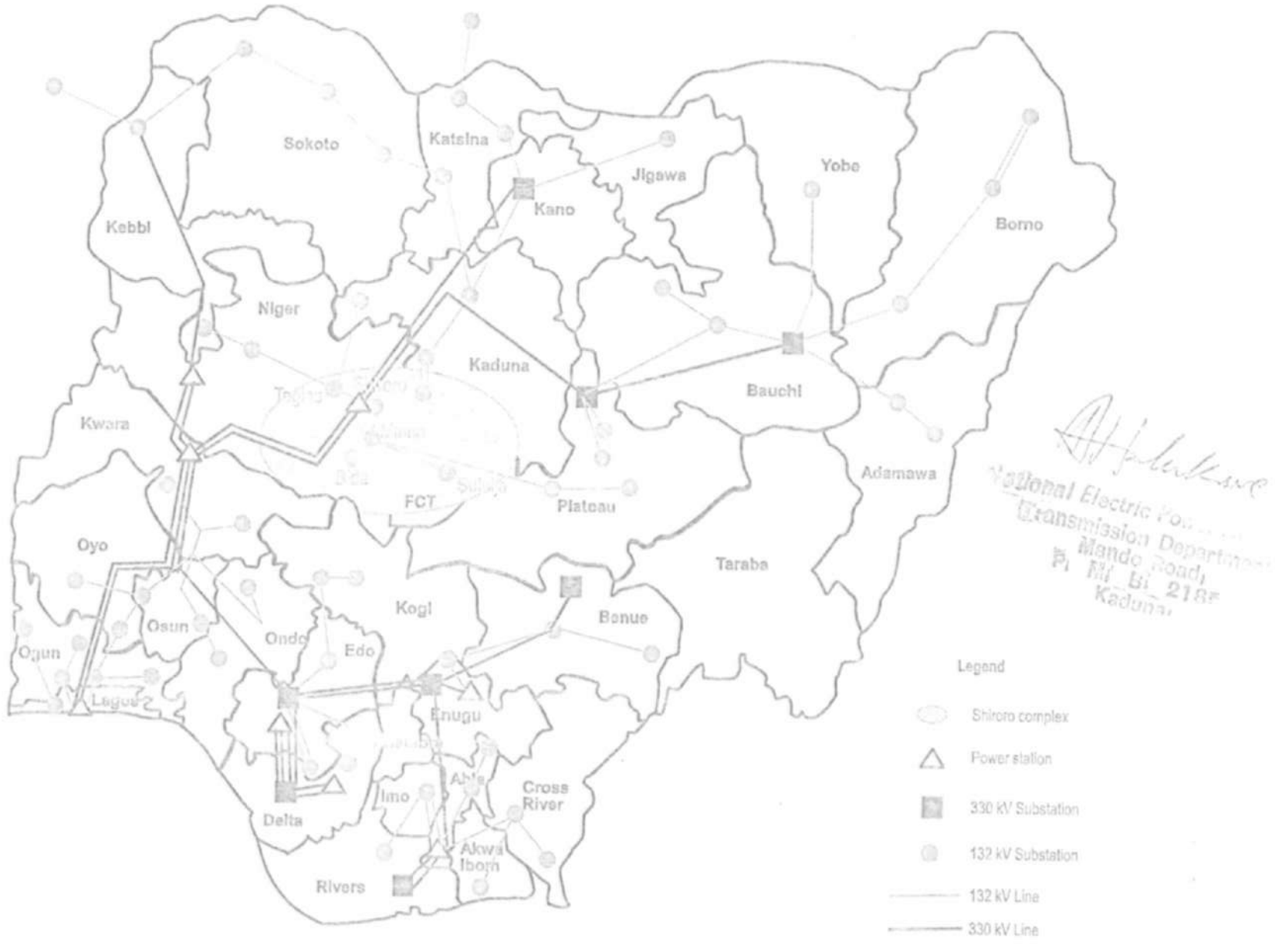
```
      SUBROUTINE LUBKSB(A,N,NP,INDX,B)
      DIMENSION A(NP,NP),INDX(N),B(N)
      II=0
      DO 12 I=1,N
      LL=INDX(I)
      SUM=B(LL)
      B(LL)=B(I)
      IF(II.NE.0.) THEN
      DO 11 J=II,I-1
      SUM=SUM-A(I,J)*B(J)
   11 CONTINUE
      ELSE IF(SUM.NE.0.) THEN
      II=I
      END IF
      B(I)=SUM
   12 CONTINUE
      DO 14 I=N,1,-1
      SUM=B(I)
      DO 13 J=I+1,N
      SUM=SUM-A(I,J)*B(J)
   13 CONTINUE
      B(I)=SUM/A(I,I)
   14 CONTINUE
      RETURN
      END
```

```
      SUBROUTINE MATMUL(PC,ADMAT,Z,M)
      DO 63 K=1,M
      PC(I,J)=0.
      DO 62 I=1,M
      DO 62 J=1,M
      PC(I,J)=PC(I,J)+ADMAT(I,J)*Z(I,J)
   62 CONTINUE
   63 CONTINUE
      DO 64 I=1,M
      DO 64 J=1,M
      A(I,J)=PC(I,J)
   64 CONTINUE
      RETURN
      END
```

```
      SUBROUTINE JACOBI(A,N,NP,D,V,NROT)
      PARAMETER(NMAX=100)
      DIMENSION A(NP,NP),D(NP),V(NP,NP),B(NMAX),Z(NMAX)
      COMPLEX GAMMA,BETAA
      DO 12 IP=1,N
      DO 11 IQ=1,N
      V(IP,IQ)=0
   11 CONTINUE
      V(IP,IQ)=1
   12 CONTINUE
      DO 13 IP=1,N
      B(IP)=A(IP,IP)
      D(IP)=B(IP)
      Z(IP)=0
   13 CONTINUE
      NROT=0
      DO 24 I=1,50
      SM=0
      DO 15 IP=1,N-1
      DO 14 IQ=IP+1,N
      SM=SM+ABS(A(IP,IQ))
   14 CONTINUE
   15 CONTINUE
      IF(SM.EQ.0.) RETURN
      IF(I.LT.4) THEN
      TRESH=0.2*SM/N**2
      ELSE
      TRESH=0
      END IF
      DO 22 IP=1,N-1
      DO 21 IQ=IP+1,N
      G=100.*ABS(A(IP,IQ))
      IF(I.GT.4).AND.(ABS(D(IP))+G.EQ.ABS(D(IP))).AND.(ABS(D(IQ))+G.EQ.A
     KBS(D(IP))) THEN
      A(IP,IQ)=0
      ELSE IF(ABS(A(IP,IQ)).GT.TRESH) THEN
      H=D(IQ)-D(IP)
      IF(ABS(H)+G.EQ.ABS(H)) THEN
      T=A(IP,IQ)/H
      ELSE
      THET=0.5*H/A(IP,IQ)
      T=1./(ABS(THET)+SQRT(1.+THET**2))
      IF(THET.LT.0.) T=-T
      END IF
      C=1./SQRT(1+T**2)
      S=T*C
      TAU=S/(1+C)
      H=T*A(IP,IQ)
      Z(IP)=Z(IP)-H
      Z(IQ)=Z(IQ)+H
      D(IP)=D(IP)-H
      D(IQ)=D(IQ)+H
      A(IP,IQ)=0.
      DO 16 J=IP-1
      G=A(J,IP)
      H=A(J,IQ)
      A(J,IP)=G-S*(H+G*TAU)
      A(J,IQ)=H+S*(G-H*TAU)
   16 CONTINUE
      DO 17 J=IP+1,IQ-1
```

```
      G=A(IP,J)
      H=A(J,IQ)
      A(IP,J)=G-S*(H+G*TAU)
      A(J,IQ)=H+S*(G-H*TAU)
   17 CONTINUE
      DO 18 J=IQ+1,N
      G=A(IP,J)
      H=(IQ,J)
      A(IP,J)=G-S*(H+G*TAU)
      A(IQ,J)=H+S*(G-H*TAU)
   18 CONTINUE
      DO 19 J=1,N
      G=V(J,IP)
      H=V(J,IQ)
      V(J,IP)=G-S*(H+G*TAU)
      V(J,IQ)=H+S*(G-H*TAU)
   19 CONTINUE
      NROT=NROT+1
   21 CONTINUE
   22 CONTINUE
      DO 23 IP=1,N
      B(IP)=B(IP)+Z(IP)
      D(IP)=B(IP)
      Q=V(IP,IQ)
      GAMMA=SQRT(D(IP))
      ALPHAA=REAL(GAMMA)
      BETAA=IMAG(GAMMA)
      IF(BETAA.EQ.0.) RETURN
      ELSE
      MUU=OMEGA/BETAA
      Z(IP)=0.
   23 CONTINUE
   24 CONTINUE
      PAUSE '50 iterations should never happen'
      RETURN
      END


      SUBROUTINE REAG(C,XG)
      DIMENSION C(N,N),XG(N,N)
      DO 40 I=1,N
      DO 40 J=1,N
      XG=OMEGA*MU*C(I,J)/(2.*PI)
   40 CONTINUE
      RETURN
      END
```



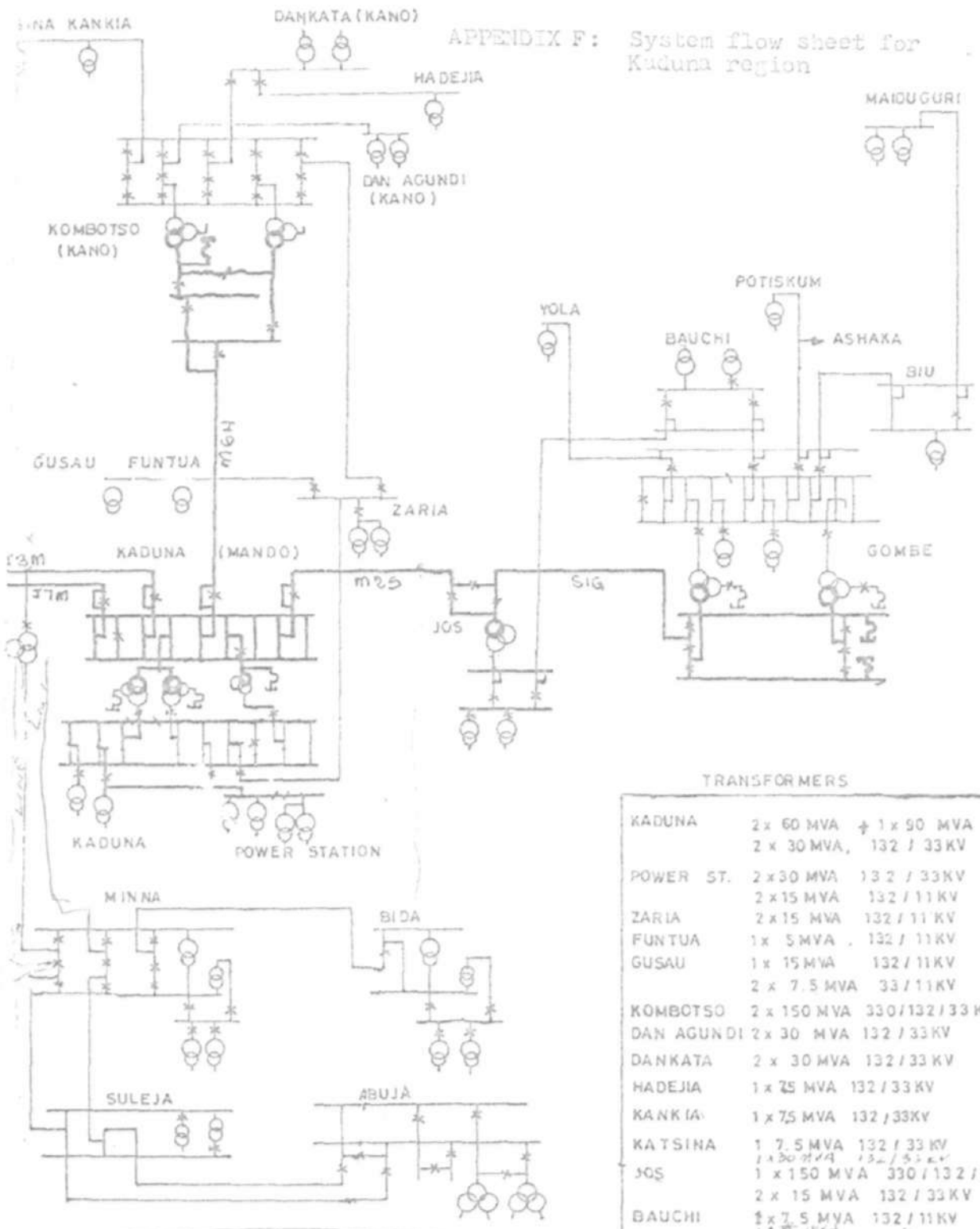

National Electric Power
Transmission Department
Mando Road,
P. M. B. 2187
Kaduna.

Appendix E: Map of Nigeria showing the NEPA grid system (Shiroro complex highlighted)

SYSTEM FLOW SHEET - KADUNA REGION

N E P A KADUNA

APPENDIX F: System flow sheet for Kaduna region




TRANSFORMERS

| | |
|---|---|
| KADUNA | 2 x 60 MVA + 1 x 90 MVA 330 / 132 KV<br>2 x 30 MVA, 132 / 33 KV |
| POWER ST. | 2 x 30 MVA 132 / 33 KV<br>2 x 15 MVA 132 / 11 KV |
| ZARIA | 2 x 15 MVA 132 / 11 KV |
| FUNTUA | 1 x 5 MVA . 132 / 11 KV |
| GUSAU | 1 x 15 MVA 132 / 11 KV<br>2 x 7.5 MVA 33 / 11 KV |
| KOMBOTSO | 2 x 150 MVA 330/132/33 KV |
| DAN AGUNDI | 2 x 30 MVA 132 / 33 KV |
| DANKATA | 2 x 30 MVA 132 / 33 KV |
| HADEJIA | 1 x 7.5 MVA 132 / 33 KV |
| KANKIA | 1 x 7.5 MVA 132 / 33 KV |
| KATSINA | 1 7.5 MVA 132 / 33 KV |
| JOS | 1 x 150 MVA 330 / 132 / 33 KV<br>2 x 15 MVA 132 / 33 KV |
| BAUCHI | 1 x 7.5 MVA 132 / 11 KV |
| GOMBE | 2 x 150 MVA 330 / 132 / 33 KV<br>2 x 15 MVA 132 / 33 KV |
| BIU | 1 x 7.5 MVA 132 / 33 KV |
| MAIDUGURI | 2 x 15 MVA 132 / 11 KV |
| POTISKUM | 1 x 5 MVA 132 / 33 KV |
| YOLA | 1 x 7.5 MVA 132 / 11 KV |
| SHIRORO | 1 x 90 MVA 330 / 133 / 13.8 KV |
| [illegible] | 2 x 30 MVA 132 / 33 KV<br>2 x 15 MVA [illegible] |
| BIDA | 2 x 30 MVA 132 / 33 KV<br>2 x 15 MVA 33 / 11 KV |
| SULEJA | 2 x 7.5 MVA 132 / 11 KV |
| ABUJA | 2 x 45 MVA 132 / 33 / 11 KV |

SHIRORO [illegible] CENTRE

33 KV Lines

132 KV Minna / Suleja / Abuja line I

132 KV Minna - Suleja - Abuja line II

132 KV Minna - Bida line

132 KV Shiroro - Tegina line (4 [illegible])